PHYSICAL REVIEW D **77,** 034022 (2008)

Color-transfer enhancement for heavy quarkonium production

Gouranga C. Nayak,[1,2] Jian-Wei Qiu,[3,4] and George Sterman[1]

[1]*C. N. Yang Institute for Theoretical Physics, Stony Brook University, SUNY, Stony Brook, New York 11794-3840, USA*

[2]*Department of Physics, University of Illinois, Chicago, Illinois 60607, USA*

[3]*Department of Physics and Astronomy, Iowa State University, Ames, Iowa 50011, USA*

[4]*High Energy Physics Division, Argonne National Laboratory, Argonne, Illinois 60439, USA*

(Received 26 November 2007; published 27 February 2008)

We study the transfer of color between a heavy quark pair and an unpaired heavy quark or antiquark moving at a nonrelativistic velocity with respect to the pair. We find that the open heavy quark or antiquark can catalyze the transformation of the pair from octet representation at short distances to singlet at long distances. This process is infrared sensitive in general, and we exhibit double poles in dimensional regularization at next-to-next-to-leading order in the transition probability. Because of their dependence on kinematic variables, these poles cannot be matched to the nonperturbative matrix elements of effective field theories based on a single heavy quark pair.

DOI: 10.1103/PhysRevD.77.034022 PACS numbers: 12.38.Bx, 12.39.St, 13.87.Fh, 14.40.Gx

I. INTRODUCTION

Heavy quarkonium production is of special interest in quantum chromodynamics (QCD), because the formation of the heavy quark pair leading up to its hadronization can be perturbative. The subsequent evolution of the pair has been extensively and fruitfully treated in the language of effective theories. Prominent among these are nonrelativistic QCD (NRQCD) [1–4] and its extensions [5–7]. In NRQCD, the nonperturbative dynamics is organized through matrix elements of operators that are characterized by an expansion in v, the relative velocity of the pair.

The NRQCD expansion in v is well understood for heavy quarkonium decays [1], although it still lacks a fully compelling proof for production processes. The NRQCD expansion, however, should not be expected to apply to reactions in which three heavy particles, two quarks and an antiquark, for example, are produced close together in phase space, because in such cases there is no unique choice of relative velocity v. In this paper, we will extend the reasoning of Ref. [8], and argue that in this limited region of phase space, the formation of color-singlet quark pairs may be enhanced by a process that we will refer to below as color transfer.

The application of NRQCD to production processes has had many successes [2–4,9]. There are, however, problematic cases. One involves the polarization of high-p_T charmonia as observed at the Tevatron [10,11]. In connection with these data, the importance of associated production within the formalism of leading-order (LO) NRQCD has recently been shown in Ref. [12]. Another unexpected observation was the large production cross section for J/ψ in association with $c\bar{c}$ pairs, as seen by the BELLE and *BABAR* collaborations [13]. It has been shown that much of this excess may be accounted for within NRQCD by computing next-to-leading-order (NLO) corrections [14].

The discussion below will explore the possibility that a complete picture for associated production will require us to extend NRQCD itself. We will argue that associated production with J/ψ and related quarkonium states may be sensitive to the kinematic region mentioned above, where heavy quarkonium is produced close in phase space to an open heavy flavor meson. The additional quark, itself a source of color, could influence the hadronization of these states. This mechanism also sheds light on NRQCD factorization [15] for processes without associated heavy quark pairs, and we will make contact with our previous work on that important question [16,17].

In the following section, we begin with a discussion of infrared poles in dimensional regularization for NLO corrections to associated production in e^+e^- annihilation [14]. We will exhibit infrared divergences that, although purely imaginary at this order, do not match with NRQCD operator matrix elements. These infrared poles are associated with the transfer of color between two heavy quarks and an antiquark, and cannot be associated with a quarkonium wave function. In Sec. III, we analyze these NLO corrections in the limit that the relative velocity for one quark-antiquark combination is much smaller than that of the other, while both velocities are nonrelativistic. In this nonrelativistic, velocity-ordered region, we will exhibit an infrared divergence with a characteristic kinematic enhancement. We will go on to identify the effective nonlocal operator that generates the leading contribution, and relate it to a similar combination encountered in the effective theory known as potential NRQCD [5].

Section IV treats this color-transfer effect at next-to-next-to-leading order (NNLO) in the velocity-ordered region. We find in this case a real contribution to the cross section with a double infrared pole. Generalizing this purely perturbative result, in Sec. V we motivate an order-of-magnitude estimate for the color-transfer contribution to the cross section. We provide numerical estimates at B factory energies, which suggest that color transfer can be competitive with the familiar color-singlet mechanism for associated production.

We go on in Sec. VI to study briefly the high-energy behavior of the color-transfer mechanism. Although we use the example of e^+e^- annihilation, many of our observations apply as well to fragmentation in hadronic collisions. We exhibit why, as already found in [12], associated production is leading power in transverse momentum for the low relative velocity region that we have in mind. We also touch on issues of polarization at high energy. We conclude with a summary that suggests directions for future work.

II. NRQCD MATCHING AND NLO CORRECTIONS

Nonrelativistic QCD organizes production and decay probabilities in terms of an expansion in the relative velocity, $v \ll 1$, of the quark-antiquark pair that eventually forms the bound state. In associated production, final states have two pairs. We will refer to the pair that eventually forms the bound state as the ''active'' pair. We will refer to the additional heavy particle that is closest in phase space to the active pair as the ''spectator'' quark (or antiquark).

The quark and antiquark momenta of the active pair are P_1 and P_2, respectively. These momenta are related to the total and relative momenta and their rest-frame relative velocity by

$$P_1 = \frac{P}{2} + q, \qquad P_2 = \frac{P}{2} - q,$$
$$v^2 = \frac{q^2}{E^{*2}} = 1 - \frac{4m^2}{P^2}. \tag{1}$$

Here $2E^*$ is the total energy of the active pair in the pair rest frame, and the second expression for v gives its relation to the quark mass and the invariant mass of the pair.

Our discussion in this section will lead to a direct evaluation of familiar one-loop diagrams in the eikonal approximation, which will be followed in a later section by an analysis of the infrared behavior of all relevant two-loop corrections. In essence, we will supplement below the calculations of Refs. [16,17], by studying infrared poles in corrections to the production of a heavy quark pair due to the exchange of soft gluons with an additional *massive* final-state particle. The extension from massless to massive particles in the final state has important consequences for a cross section in which the color of the quark pair is fixed to be in a singlet configuration in the final state. When other massive particles are observed, double infrared poles in dimensional regularization that are absent in the massless case appear in NRQCD coefficient functions. These poles have residues that depend sensitively on the relative momenta of the pair and the heavy particles. They are sharply peaked at small relative momentum, but fall off very rapidly when the relative momentum exceeds the masses.

A. Lowest order and NRQCD

Figure 1 shows the lowest-order diagrams that contribute to associated production in $e^+e^- \to Q\bar{Q} + Q\bar{Q}$ annihilation through a virtual photon. To form a heavy quarkonium state, it is assumed that the members of the active pair are close together in phase space, with relative velocity $v \ll 1$ in Eq. (1).

To derive the NRQCD expression for the production of heavy quarkonium H corresponding to the diagrams of Fig. 1, we first project these amplitudes onto a complete set of spin, angular momentum, and color states, collectively labeled n, for the pair. We then square these amplitudes, normalize appropriately, and multiply each of the resulting expressions by the corresponding NRQCD matrix elements, which summarize nonperturbative dynamics. Summing over n, we have, schematically,

$$d\sigma_{e^+e^-\to H+X}(p_H) = \sum_n d\hat{\sigma}^{(\mathrm{LO})}_{e^+e^-\to Q\bar{Q}[n]+X}(p_H)\langle 0|\mathcal{O}^H_n|0\rangle, \tag{2}$$

with p_H the quarkonium momentum. Color-singlet NRQCD operators are of the general form [1]

$$\mathcal{O}^H_{n(1)}(0) = \sum_N \chi^\dagger(0)\kappa_{n(1)}\psi(0)|N, H\rangle\langle N, H|\psi^\dagger(0)\kappa'_{n(1)}\chi(0)$$
$$= \chi^\dagger(0)\kappa_{n(1)}\psi(0)(a^\dagger_H a_H)\psi^\dagger(0)\kappa'_{n(1)}\chi(0), \tag{3}$$

with κ_n and κ'_n projections for color (octet or singlet) and

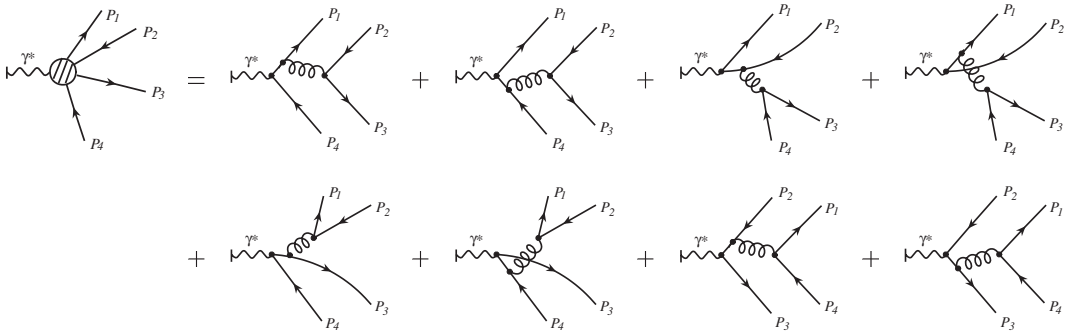

FIG. 1. The LO diagrams for a virtual photon decaying into two heavy quark pairs, at fixed quark momentum P_1 and antiquark momentum P_2. The pair P_1 and P_2 will be associated with a bound state.

spin. For this factorization to be useful, it is necessary that the "coefficient function" $d\hat{\sigma}_{e^+e^-\to Q\bar{Q}[n]+X}(p_H)$ be infrared safe at higher orders. This factorization remains a conjecture for production processes beyond NNLO.

In Ref. [16] we showed that, beyond NLO, factorization requires a reformulation of octet production matrix elements into a "gauge-completed" form,

$$\mathcal{O}^H_{n(8)}(0) = \chi^\dagger(0)\kappa_{n(8),c}\psi(0)\Phi^{(A)\dagger}_l(\infty,0)_{cb} \times (a^\dagger_H a_H)\Phi^{(A)}_l(\infty,0)_{ba}\psi^\dagger(0)\kappa'_{n(8),a}\chi(0),$$
$$\Phi^{(A)}_l(\lambda_1,0) \equiv \mathcal{P}\exp\left[-ig\int_0^{\lambda_1} d\lambda l^\mu A_{\mu,a}(\lambda l)T^{(A)}_a\right]. \quad (4)$$

Here, as shown, $\Phi^{(A)}_l(\lambda,0)_{ab}$ is a gauge link in the adjoint representation $(a,b=1\ldots8)$ with a lightlike four-velocity l, and with $\mathcal{P}$ path ordering for the expansion in g. We showed, in particular, that gauge-completed matrix elements are independent of the direction of the gauge link, so long as l remains lightlike. We will see in the calculations that follow, however, that independence of the direction of l does not generalize to a massive color source on the right-hand side of Eq. (4). This observation will have important consequences for associated production. To see how this comes about, we turn now to soft gluon loop corrections to the lowest-order diagrams of Fig. 1.

B. NLO soft gluon corrections and matching

It would be a major undertaking to compute the full NLO corrections to the singlet NRQCD cross section for two pairs at arbitrary momenta. Nevertheless, it is relatively straightforward to check the self-consistency of the NRQCD factorization at NLO in this process. This can be done by checking that infrared poles in dimensional regularization either cancel, or can be absorbed into vacuum expectation values $\langle 0|\mathcal{O}_n|0\rangle$, thus matching full QCD to NRQCD. Matching is essentially equivalent to NRQCD factorization.

More specifically, NRQCD factorization and matching for production cross sections require the cancellation of all infrared gluons that are not "topologically factorized" into factors equivalent to the perturbative expansions of matrix elements in the effective theory [1,16]. The allowed, topologically factorized, soft gluons are those that can be absorbed either into the interaction of the active pair with "the vacuum," or that do not couple to either of the heavy quarks that form the quarkonium. In the former case, the soft gluons generically will have the interpretation of part of a nonperturbative matrix element or wave function. In the latter case, they will cancel in the inclusive cross section for fixed active-pair color representation.

Figure 2 illustrates these considerations. With P_1 and P_2 the momenta of the active pair, the diagram on the upper left of the figure shows a virtual soft gluon that is emitted from the active quark and absorbed by the active antiquark.

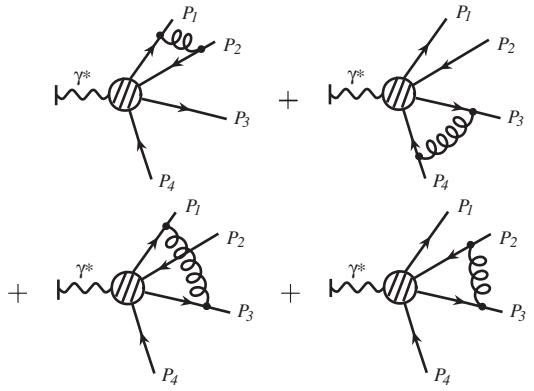

FIG. 2. Diagrams for the one-loop virtual infrared corrections, where the blob represents a complete set of lowest-order Feynman diagrams, as shown in Fig. 1.

Such a correction can be absorbed into a wave function. Similarly, contributions that describe the interference between gluon emission by the active quark in the amplitude with emission by the active antiquark in the complex conjugate amplitude are also topologically factorized, and hence consistent with NRQCD matching.

The right-hand diagram in the upper line of Fig. 2 shows a gluon that connects to neither of the active quarks. Such a contribution cancels in the sum over final states at fixed color representation of the active quarks. It is thus also consistent with NRQCD matching.

In the remaining two diagrams of Fig. 2, a member of the pair interacts with a spectator quark, of momentum P_3 in this case. These two diagrams are therefore not topologically factorized. Nevertheless, in a production cross section the real infrared poles of these diagrams still cancel against diagrams with soft gluons in the final state, for a fixed color projection on the active quark pair [1]. Of course any imaginary terms cancel upon combination with complex conjugate diagrams. At NLO, therefore, the nontopologically factored diagrams do not affect NRQCD calculations [14].

In Ref. [17], however, we found a somewhat stronger result for the imaginary poles of the nonfactored diagrams of Fig. 2. When the spectator momentum is lightlike (i.e., $P_3^2=0$), the "Coulomb phase" associated with the exchange of a soft gluon between a massive quark and a massless quark is independent of their relative directions. As a result, the imaginary infrared poles of the two nonfactored diagrams in Fig. 2 differ only by a relative minus sign between the quark and antiquark in the active pair. Once we project on a singlet final color state for the pair, they then cancel identically, to *all* orders in the relative velocity, v, Eq. (1). This is an important ingredient in the NNLO factorization of gauge-completed octet NRQCD matrix elements, Eq. (4).

We will reproduce these diagrammatic results below, but show that they no longer hold for a massive spectator (anti)quark. For a massive spectator, the infrared pole is a

simple but nontrivial function of the pair relative velocity v, as well as the pair-spectator relative velocity.

At the level of infrared poles in dimensional regularization, the one-loop virtual corrections for the diagrams shown in Fig. 2 can be factorized into LO short-distance color matrices, $M^{(\mathrm{LO})}$, times long-distance color matrices, which describe the exchange of soft gluons. The latter can be calculated in the eikonal approximation, in which the jth quark or antiquark propagator and vertex are replaced by the spin-independent combination

$$\pm\, g\,\frac{P_j^{\mu}}{P_j\cdot k}\,(T_a^{(f)})_{i_j;i'_j}, \tag{5}$$

with the plus sign for a quark and the minus for an antiquark, and where $f = q$ or $\bar{q}$ denotes the quark or antiquark representation for the generators $T_a^{(f)}$. Equivalently, we may take all color matrices in the defining (quark) representation, and stipulate that matrix multiplication follows the arrows that represent the flow of fermion number.

In these terms we write the factorized amplitude as

$$A^{(\mathrm{NLO,IR})}_{i_3 i_4} = \sum_{i'_1\ldots i'_4} \delta_{i_1 i_2}\,\mathcal{A}^{(1)}_{i_1\ldots i_4;i'_1\ldots i'_4}(P_1,P_2;P_3,P_4) \times M^{(\mathrm{LO})}_{i'_1\ldots i'_4}(P_1,P_2;P_3,P_4), \tag{6}$$

where $M^{(\mathrm{LO})}$ is the leading-order amplitude projected on the appropriate spin state, at fixed values of color indices. $\mathcal{A}^{(1)}$ is the eikonal factor, describing the coupling of a soft gluon to the outgoing quarks. The diagrams of Fig. 3 are typical contributions to $\mathcal{A}^{(1)}$, and in this case correspond to the nonfactored diagrams in Fig. 2, with the heavy lines representing the eikonal approximation (5) for the couplings of soft gluons of momentum k.

In Eq. (6), color indices i_1 and i_2 correspond to the active pair, of momenta P_1 and P_2, which are associated with the heavy quarkonium. As shown, we set $i_1 = i_2$ and sum to enforce a color-singlet final state. The remaining color indices i_3 and i_4 correspond to the open heavy quark pair, of momenta P_3 and P_4, as shown in Fig. 1. We now turn to the evaluation of the nonfactored contributions.

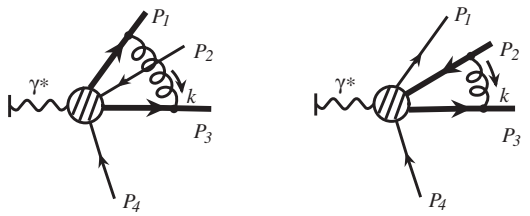

FIG. 3. Diagrams with eikonal interactions between the heavy quark pair and an associated heavy quark of momentum P_3. The heavy lines indicate fermions in the eikonal approximation.

C. Infrared poles in the NLO amplitude

The contributions of the two diagrams in Fig. 3 to the eikonal factor in Eq. (6) are given in $D = 4 - 2\varepsilon$ dimensions by

$$\begin{aligned}
[\mathcal{A}_{13}]_{i_1\ldots i_4;i'_1\ldots i'_4} &= -ig^2\mu^{2\varepsilon}(T_a^{(q)})_{i_1 i'_1} \times (T_a^{(q)})_{i_3 i'_3}\,\delta_{i_2 i'_2}\,\delta_{i_4 i'_4}\int\frac{d^Dk}{(2\pi)^D} \times \frac{P_1\cdot P_3}{[P_1\cdot k+i\epsilon][-P_3\cdot k+i\epsilon][k^2+i\epsilon]},\\
[\mathcal{A}_{23}]_{i_1\ldots i_4;i'_1\ldots i'_4} &= -ig^2\mu^{2\varepsilon}(-T_a^{(q)*})_{i_2 i'_2} \times (T_a^{(q)})_{i_3 i'_3}\,\delta_{i_1 i'_1}\,\delta_{i_4 i'_4}\int\frac{d^Dk}{(2\pi)^D} \times \frac{P_2\cdot P_3}{[P_2\cdot k+i\epsilon][-P_3\cdot k+i\epsilon][k^2+i\epsilon]},
\end{aligned} \tag{7}$$

with $\mathcal{A} = \mathcal{A}_{13} + \mathcal{A}_{23} + \ldots$. For the analysis of this section, we will assume equal masses $m = \sqrt{P_1^2} = \sqrt{P_2^2}$ for the active quark pair, but allow the additional heavy flavor to have a possibly different but nonzero mass, $m_3 = \sqrt{P_3^2}$.

In accordance with our previous discussion, we will be interested in the relative motion of the three heavy particles. For the equal-mass case, a convenient choice for relative velocity between P_i and P_j is $\beta_{ij} = \sqrt{1-4m^2/s_{ij}}$, where we adopt the notation

$$s_{ij} = (P_i + P_j)^2. \tag{8}$$

As in Eq. (1), we define $v = \beta_{12}$ for the relative velocity between the active pair. Consider now momenta p and p' with arbitrary masses, m and m'. Their relative velocity in any frame where their spatial components are collinear is given by

$$\beta(p,p') = |\mathbf{v}-\mathbf{v}'|_{\mathrm{col}} = \frac{1}{EE'}\sqrt{(p\cdot p')^2-(mm')^2}, \tag{9}$$

where $E = p_0$, and similarly for E' in the same frame. For equal masses and in the center-of-mass frame, $\beta(P_i,P_j)$ reduces to twice the familiar relative velocity, $\sqrt{1-4m^2/s_{ij}}$, of Eq. (1).

Another measure of the distance in phase space between two vectors that arises in the soft gluon corrections at hand is

$$\bar{\beta}(p,p') = \frac{EE'}{p\cdot p'}\,\beta(p,p') = \sqrt{1-\frac{m^2m'^2}{(p\cdot p')^2}}. \tag{10}$$

We easily verify the limiting behaviors,

$$\lim_{(mm')/(p\cdot p')\to 1} \bar{\beta}(p,p') = \beta(p,p'),$$
$$\lim_{(mm')/(p\cdot p')\to 0} \bar{\beta}(p,p') = \frac{1}{2}\beta(p,p'). \tag{11}$$

That is, for small relative velocities, $\bar{\beta}$ is nearly equal to β, although it increases somewhat more slowly with center-of-mass momenta, reaching a limit of $\bar{\beta}\sim 1$ for fully relativistic motion. We will be interested in regions of phase space for which relative velocities are nonrelativistic. In such regions, $\bar{\beta}$, $\beta \ll 1$. For convenience, we will refer to $\bar{\beta}$ as a velocity.

So that we may unambiguously distinguish the spectator quark, we restrict ourselves to momenta for which $v < \bar{\beta} \ll 1$. In this region of phase space, conventional NRQCD factorization need not apply directly, because of the presence of an additional small parameter, $\bar{\beta}$. Indeed, we will find an additional infrared-sensitive enhancement in the octet-to-singlet conversion for the active quark pair, due to the presence of a nearby spectator. If this mechanism is observable, it should manifest itself as a peak in open heavy-flavor meson distributions in phase space near quarkonia.

The evaluation of each integral in Eq. (7) is reasonably straightforward, and we readily isolate their infrared poles. In fact, in dimensional regularization these integrals vanish through the cancellation of IR and UV poles. Nevertheless, the single infrared pole may be found (for example) by adding quadratic terms $+k^2/2$ to the eikonal denominators. The result is

$$\mathrm{Pole}^{(\mathrm{IR})}\left[-ig^2\int\frac{d^Dk}{(2\pi)^D}\frac{P_i\cdot P_j}{[P_i\cdot k+i\epsilon][-P_j\cdot k+i\epsilon][k^2+i\epsilon]}\right]$$
$$=-\frac{1}{2\epsilon}\frac{\alpha_s}{2\pi}\frac{1}{\bar{\beta}(P_i,P_j)}\left(\ln\left[\frac{1+\bar{\beta}(P_i,P_j)}{1-\bar{\beta}(P_i,P_j)}\right]-2i\pi\right), \tag{12}$$

where $\bar{\beta}$ has been defined in (10). In the region that we have identified above, $\bar{\beta}(P_i,P_j)\ll 1$, we observe that, for the infrared pole, singular behavior in $\bar{\beta}$ appears in the imaginary, but not in the real part,

$$\mathrm{Pole}^{(\mathrm{IR})}\left[-ig^2\int\frac{d^Dk}{(2\pi)^D}\frac{P_i\cdot P_j}{[P_i\cdot k+i\epsilon][-P_j\cdot k+i\epsilon][k^2+i\epsilon]}\right]$$
$$=-\frac{1}{\epsilon}\frac{\alpha_s}{2\pi}\frac{1}{\bar{\beta}(P_i,P_j)}(\bar{\beta}(P_i,P_j)-i\pi)+\mathcal{O}(\bar{\beta}(P_i,P_j)). \tag{13}$$

Our discussion below will concentrate on the effect of this pole on production cross sections, which, as we shall show, is seen first at NNLO.

At this point we note that the real part of the full vertex correction has a (famous) $1/\bar{\beta}$ singularity. This power singularity near threshold, however, is finite in four dimensions, and is associated with loop momenta at the scale of mv^2, the so-called "ultrasoft" momenta. Dynamics at this scale are regulated by bound-state effects between the active quarks. In this paper, we shall not attempt an analysis of exchanges at the ultrasoft scale between the active pair and spectators.

Consider now the imaginary contributions of Eq. (7) to $\mathcal{A}$, traced over the colors of the active pair to enforce a singlet configuration in the final state,

$$\sum_{i_1 i_2}\delta_{i_1 i_2}\mathrm{Im}[\mathcal{A}_{13}+\mathcal{A}_{23}]_{i_1\ldots i_4;i_1'\ldots i_4'}$$
$$=\frac{1}{\epsilon}\left(\frac{\alpha_s}{2}\right)(T_a)_{i_2' i_1'}(T_a)_{i_3 i_3'}\delta_{i_4 i_4'}\left[\frac{1}{\sqrt{1-P_1^2P_3^2/(P_1\cdot P_3)^2}}\right.$$
$$\left.-\frac{1}{\sqrt{1-P_2^2P_3^2/(P_2\cdot P_3)^2}}\right]. \tag{14}$$

This pole in the imaginary part vanishes identically for $P_1\cdot P_3 = P_2\cdot P_3$ or for $P_3^2=0$. In the former case, the relative velocity of the spectator quark and the active quark equals the relative velocity of the spectator and the active antiquark. The interpretation of the cancellation is then that soft gluons emitted by the spectator cannot resolve the charges of a perfectly comoving pair in a singlet color state. Analogously, when the spectator is lightlike, the relative velocity to both active lines is unity, and the two terms cancel. Evidently, in this case a lightlike spectator cannot resolve a color singlet even when the quark and antiquark are not comoving.

From Eq. (14), the sum of the exchanges between the active pair and the spectator depends directly on the relative velocities of the spectator with the active quark and antiquark, but only indirectly on the relative velocity v of the active pair itself. In general, for $\beta_{13}\sim\beta_{23}$, we must describe the kinematics of two quarks vying for the favor of a single antiquark to form a heavy bound state, with no obvious favorite. This three-body problem is potentially difficult to analyze. The soft gluon dynamics of two quarks and an antiquark might be generated from local operators like $\psi^\dagger_{P_1}\chi_{P_2}\psi^\dagger_{P_3}$, with time evolution generated by heavy quark effective theory for each of the quarks, but only if we neglect the recoil of the quarks. Nonrelativistic QCD organizes such corrections into nonperturbative matrix elements, but only to the extent that the extra quark may be neglected.

We will not attempt a full solution to the three-particle problem, but will concentrate in the following on a limit more closely related to NRQCD. We have already noted that the sum of NLO phases in Eq. (14) vanishes in the limit $v=\beta_{12}\to 0$, at fixed, finite values of $\bar{\beta}_{13}=\bar{\beta}_{23}$. We now turn to this region of nonrelativistic, ordered velocities, which we will refer to as the "velocity-ordered region."

III. NLO COLOR TRANSFER FOR ORDERED VELOCITIES

We begin this section by expanding the residue of the infrared pole on the right-hand side of Eq. (14) to lowest

order in the active-pair relative velocity, v, in the velocity-ordered region. The residue is strongly peaked toward low relative velocity for the spectator pair. We will then go on to rederive this result from an effective nonlocal vertex involving the gluon field strength coupled to the dipole moment of the active pair [16]. This reformulation will enable us to extend our analysis to NNLO in the following section, and also to exhibit the relation of the analysis here to our previous study of NRQCD factorization [17] and to potential NRQCD [5].

A. Expansion in v

To estimate the kinematic behavior of the poles in Eq. (14) in the velocity-ordered region, we expand at low relative velocity v for the active pair. In Eq. (14), the only kinematic variables are $P_1 \cdot P_3$ and $P_2 \cdot P_3$, and we expand both around their values at $v = 0$, $(P/2) \cdot P_3$, with $P^2 = 4m^2$ We will allow P_3 to have an arbitrary nonzero mass, m_3. Given that we have two invariants, we will have to introduce an additional relative velocity, and corresponding relative momentum.

We begin this straightforward kinematic analysis with Eq. (1) for the momenta of the active pair, recalling that the mass-shell conditions $P_1^2 = P_2^2 = m^2$ require $q \cdot P = 0$. In a frame where the total pair momentum is at rest, the relative momentum q^μ has no time component. We can then write the total energy of the pair as a function of q, in terms of a momentum at rest in that frame, $P_0^\mu = (2m, \vec{0})$. In covariant form the dependence of P on q is given explicitly by

$$P^\mu = P_0^\mu \sqrt{1 - \frac{q^2}{m^2}}, \tag{15}$$

where $q^2 = -\vec{q}^{\,2}_{\rm c.m.}$. We now parametrize P_3^μ in a similar way, expanding around $P_3 = (m_3, \vec{0})$ in the P^μ (active-pair) rest frame, in terms of a vector q_S^μ, which like q has a vanishing time component in that frame,

$$P_3^\mu = m_3 \frac{P_0^\mu}{2m} \sqrt{1 - \frac{q_S^2}{m_3^2}} + q_S^\mu, \quad q_S \cdot P_0 = 0. \tag{16}$$

Expressing P_3 in these terms, and recalling that $P_1 = P/2 + q$, we evaluate the relevant invariant $P_1 \cdot P_3$ as a function of q and q_S, finding

$$P_1 \cdot P_3 = m m_3 \sqrt{\left(1 - \frac{q^2}{m^2}\right)\left(1 - \frac{q_S^2}{m_3^2}\right)} + q \cdot q_S. \tag{17}$$

The analogous result for $P_2 \cdot P_3$ is found by simply changing the sign of $q \cdot q_S$. We are now ready to expand (14) in q at fixed q_S.

Starting at $q = 0$, $P_1 = P_2 = P_0/2$, both invariants $P_i \cdot P_3$, $i = 1, 2$ are given by

$$(P_0/2) \cdot P_3 = m\sqrt{m_3^2 - q_S^2} \equiv \frac{m m_3}{\sqrt{1 - \bar{\beta}_S^2}}, \tag{18}$$

where in the second expression we recall the definition of the function $\bar{\beta}$, Eq. (10), and define

$$\bar{\beta}_S \equiv \bar{\beta}(P_0/2, P_3) = \sqrt{\frac{-q_S^2}{m_3^2 - q_S^2}}. \tag{19}$$

This is a measure of the spectator's velocity relative to the active pair, neglecting the latter's internal relative velocity, v. We note that this particular velocity is independent of m, so that, for example, $\bar{\beta}(P_0/2, P_3) = \bar{\beta}(P_0, P_3)$, and $\bar{\beta}_S = 1$ for $m_3 = 0$.

Following our previous discussion, we consider the region $|q^2| < |q_S^2|$, and expand in the corresponding ratios on the right-hand side of Eq. (14), keeping in mind that at $q = q_S = 0$ both terms in the difference on the right-hand side diverge. We note as well that only terms that are odd in q^μ survive in the difference. We find

$$\frac{1}{\sqrt{1 - P_1^2 P_3^2/(P_1 \cdot P_3)^2}} - \frac{1}{\sqrt{1 - P_2^2 P_3^2/(P_2 \cdot P_3)^2}} = \frac{2}{\bar{\beta}_S^3} \frac{q_S \cdot q}{m m_3} (1 - \bar{\beta}_S^2)^{3/2} \left[1 + \mathcal{O}\left(\frac{q^2}{m^2}\right)\right]. \tag{20}$$

This result is exact in q_S up to terms that are quadratic in q. Notice that it vanishes rapidly in the limit $m_3/q_S \to 0$, that is, relativistic motion for the spectator.

We can now define the velocity-ordered region as

$$\bar{\beta}_S < 1, \qquad \frac{v}{\bar{\beta}_S} < 1. \tag{21}$$

That is, we shall assume that it is possible to expand in $v/\bar{\beta}_S$, keeping in mind that not all v or $\bar{\beta}_S$ dependence is of this form. Of course, such an expansion may be of limited quantitative use when $\bar{\beta}_S \sim v$. This is a region likely to be of particular importance for charm quarks, where even v need not be small, and where the dynamics goes over into a true three-body problem. Nevertheless, we hope to gain insight even from the somewhat idealized kinematical limit of Eq. (21).

For small $\bar{\beta}_S$, Eq. (19) shows that the vector q_S is proportional to $\bar{\beta}_S$, just as the active pair's relative momentum q is proportional to v. In this way, we can rewrite our result in a form that exhibits the leading dependence on both velocities v and $\bar{\beta}_S$ in the velocity-ordered region,

$$\frac{1}{\sqrt{1 - P_1^2 P_3^2/(P_1 \cdot P_3)^2}} - \frac{1}{\sqrt{1 - P_2^2 P_3^2/(P_2 \cdot P_3)^2}} = -\frac{2}{\bar{\beta}_S^2} v \cos\phi_S \left[1 + \mathcal{O}\left(\frac{q^2}{m^2}, \frac{q \cdot q_S q_S^2}{m m_3^3}\right)\right], \tag{22}$$

where on the right ϕ_S is the angle between $\vec{q}_S$ and $\vec{q}$ in the

rest frame of the active pair. Equation (22) provides an explicit illustration of the enhancement of gluon exchange as the spectator approaches the active pair in phase space.

We can summarize our analysis for the imaginary NLO pole in the amplitude at small q_S by using (20) and (22) in (14), which gives

$$\sum_{i_1 i_2} \delta_{i_1 i_2} \mathrm{Im}[\mathcal{A}_{13} + \mathcal{A}_{23}]_{i_1 \ldots i_4; i'_1 \ldots i'_4} \sim -\frac{1}{\varepsilon}\left(\frac{\alpha_s}{2}\right)(T_a)_{i_2 i'_1}(T_a)_{i_3 i'_3}\delta_{i_4 i'_4}\frac{2}{\bar{\beta}_S^2}(1-\bar{\beta}_S^2)^{3/2} v \cos\phi_S. \tag{23}$$

We will return to this expression in Sec. V, when we discuss its possible phenomenological implications for quarkonium production in association with open heavy flavor. In the remainder of this section, we rederive the basic result (23) by expanding first at the diagrammatic level.

B. Operator interpretation and potential NRQCD

We have observed that the eikonal factor $\mathcal{A}$ of (14) vanishes at $v = 0$, that is, at vanishing active-pair relative momentum. The lowest order in v exhibits an infrared singularity characteristic of an electric dipole transition [16], although in this case the dipole is coupled to the field of a spectator rather than to an emitted gluon. The expansion of Eq. (14) shows this result at lowest order, through its linear behavior on the relative momentum q. In this section, however, we will expand the diagrams first to order q, and sketch the resulting calculation. We may think of this as the first step in the creation of an effective theory for color transfer, in the restricted region where $v < \bar{\beta}(P_1, P_3), \bar{\beta}(P_2, P_3)$.

We represent the sum of the two eikonal approximations to the coupling of a soft gluon to the active pair in the NLO eikonal factor in Fig. 4. As in Ref. [16], the double line on the right-hand side of the figure represents the combined quark pair. As we shall see, the double line and the vertex ⊗ correspond to a Wilson line in adjoint representation that terminates at the field-strength operator $P_\mu F^{\mu\nu} q_\nu$, where q is the relative momentum of Eq. (1).

Returning to the NLO integrals of Eq. (7), and recalling the relation between q^μ and v in Eq. (1), we see that an expansion in powers of v is equivalent to an expansion in q. For this purpose, we denote the spectator momentum by l,

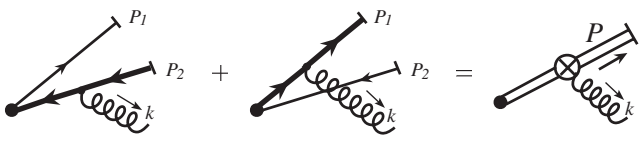

FIG. 4. Graphical representation of the first-order expansion in the relative velocity of the active pair. The vertex ⊗ represents the inner product of the chromoelectric field and the relative velocity, as in Eq. (26).

which may represent P_3 or P_4 in this case. This was the notation used in Refs. [16,17], where, however, we took $l^2 = 0$.

In these terms, the order-q correction to the two contributions to the eikonal factor $\mathcal{A}$ of Eq. (6) is given by

$$\mathcal{A}^{(1)}_{13} + \mathcal{A}^{(1)}_{23} = -ig^2\mu^{2\varepsilon}\int\frac{d^Dk}{(2\pi)^D} \times \frac{N(P,q,l,k)}{[P\cdot k + i\epsilon]^2[-l\cdot k + i\epsilon][k^2 + i\epsilon]} + \mathcal{O}\left(\frac{q^2}{P^2}\right), \tag{24}$$

where the expansion results in a squared denominator for $P \cdot k$ and in the numerator factor

$$N(P,q,l,k) = 4[q\cdot l P\cdot k - P\cdot l q\cdot k]. \tag{25}$$

As shown in Ref. [16], we can interpret this expression as the local field-strength vertex appearing in the nonlocal operator

$$E_b \equiv -ig\int_0^\infty d\lambda\lambda[P^\mu q^\nu F_{\nu\mu,a}(\lambda P)]\Phi^{(A)}_P(\lambda,0)_{ab}. \tag{26}$$

In the rest frame of the active pair, this is precisely the integral along a massive worldline, specified by momentum P, of the scalar product of the relative momentum with the electric field operator, contracted with a gauge link in adjoint representation [defined as in Eq. (4)]. Notice the factor λ in the integral, which reflects the increasing separation of the quark and antiquark as the pair propagates into the final state at fixed relative velocity $v = q/E^*$ [Eq. (1)]. The extra factor of λ produces the squared denominator in Eq. (24).

In Eq. (26), the connection of our NLO correction to the effective theory potential NRQCD (pNRQCD) [5] is manifest. The gauge link is the propagator for an octet pair in pNRQCD, and the field strength is the operator in the Hamiltonian that transforms an octet pair to a singlet configuration. Although it was not designed to describe quarkonium production, pNRQCD operators emerge naturally in the velocity-ordered region, as a description of the active pair evolving in an external color field supplied by the spectator.

We now turn to the evaluation of the NLO correction starting from the effective vertex of (26). It is straightforward to evaluate the integral in Eq. (24), but we describe it in some detail because it sheds light on the role of the spectator mass. For simplicity, we may choose $l_\perp = 0$ and $P = (M_H, \vec{0})$. From Eq. (25), we then find, after a little algebra,

$$N = 4M_H q^3[(l\cdot k) - 2l^+k^-] + 4P\cdot l q_\perp\cdot k_\perp, \tag{27}$$

where the last term vanishes after integration over $k_\perp$. The first term in square brackets, $l \cdot k$, cancels the spectator denominator. Because this term is actually independent of the spectator momentum, it can be treated in exactly the

same manner as in the massless case [17], leading to the same result. This contribution is purely real, and cancels against real-gluon emission. We are left with the contribution of the l^+k^- term only, which we now evaluate.

As in Ref. [16], we integrate over k^- first. When we close the k^- integration contour in the lower half-plane, we encounter poles from both the k^2 and $P\cdot k$ denominators. The k^2 pole gives a real result and cancels against the corresponding numerator factor for the final state with a gluon. The remaining contribution in the l^+k^- term in Eq. (24) is from the double pole at $P\cdot k=0$ in Eq. (24), which gives

$$\begin{aligned}\mathcal{A}^{(1)}_{\ell^+} &= -\frac{16g^2\mu^{2\varepsilon}}{(2\pi)^{D-1}}\left(\frac{q^3}{M_H}\right)\int_{-\infty}^{\infty}dk^+\int d^{D-2}k_\perp\frac{d}{dk^-}\left[\frac{l^+k^-}{(2k^+k^- - k_{2\perp}^2+i\epsilon)(l^-k^+ + l^+k^- - i\epsilon)}\right]_{k^-=-k^+}\\ &= \frac{16g^2\mu^{2\varepsilon}}{(2\pi)^{D-1}}\left(\frac{q^3}{M_H}\right)\int_{-\infty}^{\infty}dk^+\int d^{D-2}k_\perp\frac{l^+}{[2(k^+)^2+k_\perp^2-i\epsilon][\sqrt{2}l^3k^+ + i\epsilon]}\left[\frac{2(k^+)^2}{2(k^+)^2+k_\perp^2}+\frac{l^-}{\sqrt{2}l^3}\right].\end{aligned} \tag{28}$$

In the second equality we have taken the derivative with respect to k^-. In the resulting expression on the right, the first term in brackets vanishes, because it is odd in k^+, while the second term can be found from the pole at $k^+=0$, and has a vanishing real part. After integration over $k_\perp$, we obtain an imaginary piece for the eikonal factor,

$$-i\mathcal{A}^{(1)}_{\ell^+} = \mathrm{Im}[\mathcal{A}^{(1)}_{13}+\mathcal{A}^{(1)}_{23}] = \frac{1}{\varepsilon}(2\alpha_s)\left(\frac{q^3}{M_H}\right)\left[\frac{l^2}{(l^3)^2}\right], \tag{29}$$

found here in the $P=(M_H,\vec{0})$ frame with $\ell_\perp=0$. In a general Lorentz frame, the leading-order eikonal factor is

$$\mathrm{Im}[\mathcal{A}^{(1)}] = -\frac{1}{\varepsilon}(2\alpha_s)\frac{P^2l^2}{[(P\cdot l)^2-P^2l^2]^{3/2}}(l\cdot q). \tag{30}$$

This result, of course, agrees (up to color factors) with the expansion of Eq. (14) for the imaginary parts of the diagrams in Fig. 3. As in Eq. (14), the essential role of the spectator mass, $\sqrt{l^2}\leftrightarrow(P_3^2)^{1/2}$, is manifest. We also see that for $P\cdot l\gg l^2$, the effect decreases as $(P\cdot l)^{-3/2}$.

Having arrived at a result identical to the expansion of Eq. (14) at NLO, we are now ready to use the operator formalism to study color transfer at NNLO in the velocity-ordered region.

IV. COLOR TRANSFER AT NNLO IN THE VELOCITY-ORDERED REGION

So far, we have identified an IR pole in the NLO imaginary part of the production amplitude for a color-singlet (active) quark pair, starting from an octet pair at short distances, by using the eikonal approximation. This contribution depends on the presence of a massive source, the spectator, nearby in phase space. The spectator catalyzes the octet-to-singlet transition of the pair, in the sense that its own color representation is unchanged. The effect decreases rapidly as the relative velocity of the source approaches unity, where the amplitude is readily matched to NRQCD. On the other hand, when the relative velocity between the pair and spectator is itself nonrelativistic, the effect is potentially significant.

Following the logic of Ref. [16], we explore the implications of these infrared poles for the production rates of heavy quarkonia in association with open heavy flavor. We will work in the velocity-ordered region, (21), where the active pair's relative velocity v is even smaller than its velocity relative to the spectator. We then expand in v.

From the point of view of NRQCD, we will calculate soft gluon corrections to the coefficient function $d\hat{\sigma}_{A+B\to Q\bar{Q}[n]+X}(p_H)$ in Eq. (2), for the specific case when a pair of heavy quarks, $Q\bar{Q}[n]$, is in a singlet configuration. We will identify real infrared *double* poles in this production amplitude starting at two loops. As above, at the level of infrared poles in dimensional regularization, these can be computed using eikonal approximation, or equivalently, as vacuum expectations values of products of Wilson lines, defined in adjoint and fundamental representations as in Eq. (4).

A. Matrix elements for pair production at NNLO

Recall that Ref. [16] dealt specifically with infrared poles in fragmentation functions. The relevant eikonal production fragmentation function is given to lowest order in $q\sim mv$ by

$$\begin{aligned}\mathcal{I}_2^{(8\to1)}(P,q,\varepsilon) \equiv 2\sum_N\int_0^\infty d\lambda'\lambda'\langle 0|\Phi_l^{(A)\dagger}(\infty,0)_{bd'}\Phi_P^{(A)}(\lambda',0)^\dagger_{d'a'}[P^\mu q^\nu F_{\nu\mu,a'}(\lambda' P)]|N\rangle\\ \times\left\langle N\left|\int_0^\infty d\lambda\lambda[P^\mu q^\nu F_{\nu\mu,a}(\lambda P)]\Phi_P^{(A)}(\lambda,0)_{ad}\Phi_l^{(A)}(\infty,0)_{db}\right|0\right\rangle,\end{aligned} \tag{31}$$

with (anti-) time ordering implicit in the (complex conjugate) amplitudes. Here $\Phi_l^{(A)}$ is the same lightlike Wilson line in adjoint representation as in Eq. (4), which represents the effect of recoiling massless quanta. The other Wilson line in

adjoint representation, $\Phi_P^{(A)}$, is massive, and represents the propagation of the pair of heavy quarks as an octet. This gauge link connects the hard scattering at the origin with the field-strength tensor as in Eq. (26), which describes the absorption of the soft gluon that changes the net color of the pair from octet to singlet. We note that in this paper we choose the argument of the field strength to be $\lambda' P$, rather than $\lambda' P/2$, as in [16], which leads to an explicit factor of 2 on the right-hand side of (31).

In this section, we study an eikonal production cross section, in which the lightlike gauge link $\Phi_l^{(A)}$ of Eq. (31) is replaced by a pair of massive Wilson lines in quark and antiquark representations. These two lines are linked together by an octet short-distance vertex (the shaded circles of the figures), which matches to the adjoint representation of the line in the same direction as the total momentum, P, of the pair. Again, the adjoint Wilson line terminates at the field-strength vertex, Eq. (26),

$$\mathcal{M}_2(P,q) \equiv \sum_N \int_0^\infty d\lambda' \lambda' \langle 0|\Phi_{P_3}^{(q)\dagger}(\infty,0)_{ij'}(T_{c'})_{j'k'}\Phi_{P_4}^{(\bar{q})\dagger}(\infty,0)_{k'l}\Phi_P^{(A)\dagger}(\lambda',0)_{c'a'}[P^\mu q^\nu F_{\nu\mu,a'}(\lambda' P)]|N\rangle$$
$$\times \left\langle N \left| \int_0^\infty d\lambda' \lambda' [P^\mu q^\nu F_{\nu\mu,a}(\lambda' P)]\Phi_P^{(A)}(\lambda',0)_{ac}\Phi_{P_4}^{(\bar{q})}(\infty,0)_{lk}(T_c)_{kj}\Phi_{P_3}^{(q)}(\infty,0)_{ji} \right| 0 \right\rangle, \tag{32}$$

again with (anti-) time ordering implicit in the (complex conjugate) amplitudes. This production cross section at NLO is represented by the diagram on the left in Fig. 5. As in Fig. 4, the double line stands for the pair of heavy quarks at low relative velocity v, terminating in a singlet final state represented by the vertical line in the figure. The vertex ⊗ supplies the necessary color. We sum over all final states that include the singlet pair (P) and the antiquark line P_4.

The diagram on the left of Fig. 5 gives the entire NLO contribution to $\mathcal{M}_2$, Eq. (32). It represents the classic lowest-order octet mechanism, in which the pair in octet representation emits a single gluon and becomes a singlet. It has a single infrared pole in dimensional regularization, and is the lowest-order contribution that is matched to nonperturbative matrix elements in NRQCD [18]. At this order, the associated pair is irrelevant to the infrared structure, so long as we concentrate on octet short-distance functions.

The diagram of the same order on the right in Fig. 5 represents an interference between an octet pair produced at short distances in the amplitude and a singlet pair produced at short distances in the complex conjugate amplitude. In the amplitude, the pair is transformed into a singlet by the exchange of a soft gluon with the spectator quark line P_3. We include this interference diagram because it illustrates at NLO the cancellation of infrared poles from an on-shell gluon ($k^2 = 0$) in virtual corrections and in the final state. Both of these states are available even when the heavy active pair (double line in the figure) is fixed to be in a singlet state. After the cancellation of the real-gluon contributions, however, the imaginary pole that we studied in Sec. III above remains, and must be canceled by complex conjugate diagrams (not shown in the figure).

Although the pole we have found above at one loop is purely imaginary, it will contribute to the real part at NNLO. This pole, of course, is just the one-loop contribution to a Coulomb phase, and is guaranteed to cancel in a fully inclusive cross section. As we shall see, however, when restrictions are placed on the color of final-state pairs, as in NRQCD, this cancellation fails, in general, at NNLO.

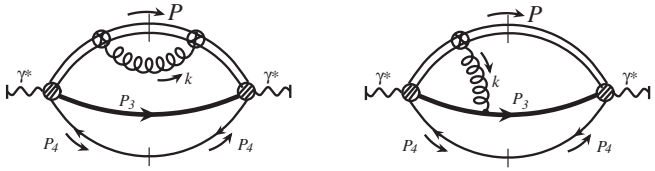

FIG. 5. NLO contributions to $\gamma^* \to [Q\bar{Q}]Q\bar{Q}$ with the double line and the vertex ⊗ defined in Fig. 4. The cut double lines in each case denote a heavy quark pair in a singlet state. The shaded circles of the diagrams represent short-distance functions in the amplitude and complex conjugate. In the figure on the left, both short-distance functions are octet, corresponding to the matrix element $\mathcal{M}_2$ of Eq. (32). In the figure on the right, the short-distance function of the amplitude is octet, and of the complex conjugate, singlet. The right-hand figure, which illustrates the cancellation of real and virtual on-shell gluons, does not correspond directly to Eq. (32).

B. The analysis of double poles at NNLO

The NNLO diagrams that contribute to the squared octet-to-singlet transition probability, Eq. (32), are shown in Fig. 6. In these diagrams, the cut double line represents the active pair in a color-singlet configuration, and the crossed circles indicate the field-strength vertices. All lines in these diagrams except for gluons are eikonal. The transition probability (32) has been constructed to reproduce the infrared behavior of diagrams in full QCD at leading order in the active-pair relative velocity, v.

The graphs shown in Fig. 6 each represent a set of cut diagrams, found by summing over all final states that include the color-singlet pair and the line P_4. As in Fig. 5, the shaded circles represent short-distance functions, which link the active pair in octet representation with the associated pair (P_3 and P_4). We work in the velocity-

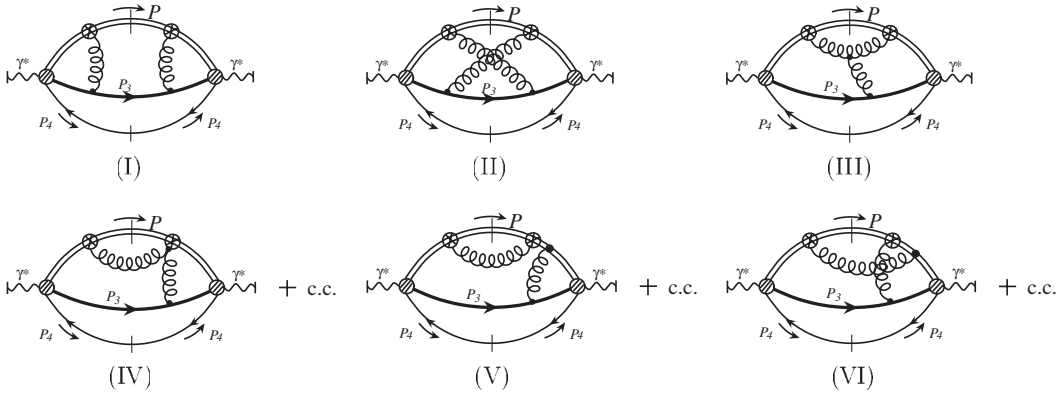

FIG. 6. Diagrams that contribute to $\mathcal{M}_2$, Eq. (32), similar to those studied in Ref. [16]. These NNLO diagrams describe the transition of a pair of momentum P from octet to singlet by the exchange of color with a spectator whose momentum, P_3, is nearby in phase space. We sum over all cuts of these diagrams that can produce a color-singlet quark pair.

ordered region, Eq. (21), and take the line labeled P_3 as the spectator that interacts with the pair. We will neglect connections of the active pair with the remaining line, P_4. That is, we assume that the relative velocity of this line to the pair is large.

Our goal in this section is to show that at NNLO there is a real infrared-sensitive contribution to the octet-to-singlet transition amplitude, $\mathcal{M}_2$. We will not calculate the diagrams explicitly, but argue that in dimensional regularization diagram (I) produces a double pole that equals the absolute square of the NLO result, Eq. (23) (up to color factors), and that there is no other source of real, double infrared poles from any other diagram. Such a real contribution to the transition amplitude cannot be matched to a local operator in NRQCD. We will rely heavily on power counting analysis, and on the specific calculations of Ref. [16].

To generate a double pole in $D = 2 - \varepsilon/2$ dimensions, a diagram must contain two momentum integrals, either virtual or real, that diverge logarithmically when $D = 4$. This can be checked by straightforward power counting. General rules for power counting estimates of infrared-sensitive diagrams are discussed, for example, in Ref. [19]. The prescription is particularly simple for massive eikonal lines exchanging gluons without gluon self-coupling vertices. This describes all the diagrams of Fig. 6 except for (III). Because all the eikonal lines are massive, there are no collinear singularities anywhere in loop momentum or phase space for diagrams (I), (II), and (IV)–(VI). In contrast, we do find collinear singularities for some momentum configurations of diagram (III) because of the three-gluon coupling in that diagram. These collinear singularities, however, cancel in the sum over cuts at fixed active-pair color by standard unitarity arguments [19], and we need not consider them here.

To perform power counting for the remaining, infrared singularities, we need to study all choices of loop momenta carried by the gluons. The momenta of the active pair is fixed, as are P_3 and P_4. When a gluon appears in the final state, we do power counting on its phase space integral, which we shall continue to refer to as a "loop" momentum. From a technical point of view, in the definition of $\mathcal{M}_2$, the vertices associated with the short-distance functions are fixed at the origin in both amplitude and complex conjugate. These vertices are therefore relatively local, and a loop momentum can begin at the short-distance function in the amplitude on the left of a diagram, and end at the short-distance function on the right, in the complex conjugate amplitude. In physical terms, because we neglect the recoil of the heavy quarks, we do not impose overall momentum conservation on soft gluons in the final state.

We scale the components of any such choice of loop momenta as

$$k_i^\mu = \lambda_i \hat{k}_i^\mu, \tag{33}$$

where $i = 1, 2$ labels a choice of loop momenta. This is just a change of variables, which will produce an overall factor λ_i^4 for each loop. When the integrand behaves as $\lambda_i^{-p_i}$ with $p_i = 4$, all sizes of loop momenta contribute equally to the result, and the integral diverges logarithmically. In fact, because these eikonal integrals are scaleless overall, there is always a single logarithmic divergence in both infrared and ultraviolet when both loops are scaled together, and the diagrams are nonzero in dimensional regularization only after imposing an ultraviolet cutoff.

The application of the scaling (33) is quite straightforward, keeping in mind several technical observations.

(1) To derive a double infrared pole, it is necessary to find logarithmic ($p_i = 4$) power counting in both the λ_i, $i = 1, 2$, individually. When any virtual eikonal line carries both loop momenta, we can neglect the dependence of that line on the softer momentum. We can thus do power counting in the softer loop alone, at fixed values of the larger loop momentum. If $p_{\text{soft}} < 4$, there is at most a single pole. On the other hand, if we find any one-loop

subdiagram with logarithmic power counting for a given final state, dimensional analysis ensures that there is a double pole.

(2) The virtual spectator eikonal lines in the P_3 direction (middle lines of the diagrams) contribute λ_i^{-1}, with i corresponding to the larger of the loop momenta that flow through the line.

(3) When there is a single active-pair eikonal line at the top of a diagram in the amplitude or complex conjugate, it gives λ_i^{-2}, with i the larger loop momentum carried by the line. The extra factor of λ_i^{-1} relative to the normal eikonal line corresponds to a modification of the standard eikonal Feynman rules [16] due to the integral that defines the adjoint eikonal (double) line ending in the field-strength vertex, Eq. (32). We have encountered this effect above in the one-loop calculation, Eq. (24). The three-point crossed vertices, however, each contribute a numerator factor of λ_i because of the linear dependence on loop momentum in their definition, and four-point crossed diagrams are independent of loop momenta. The net effect of the combination of a field-strength vertex and a single active-pair eikonal line is an overall λ_i^{-1} when a gluon of momentum k_i attaches to the vertex.

(4) When there are two active-pair eikonal lines, as in diagram (V), the diagram represents the sum of two terms, in which one of the two eikonal denominators is squared. For example, taking k_1 as the gluon connecting the field-strength vertices, and k_2 the momentum of the gluon flowing (up) from P_3 to the active eikonal in diagram (V), the two active eikonals on the right correspond to the combination

$$\frac{1}{(P\cdot k_1)^2}\,\frac{1}{P\cdot(k_1+k_2)}+\frac{1}{P\cdot k_1}\,\frac{1}{(P\cdot(k_1+k_2))^2}. \tag{34}$$

We are now ready to discuss the diagrams of Fig. 6 individually.

Diagram (IV): Let us begin the application of the above rules with diagram (IV) of Fig. 6, and show that it can generate at most a single infrared pole. We must test all independent choices of soft gluon loops. To derive a double pole, we must find one loop for which scaling according to Eq. (33) at fixed values of the other loop's momentum results in a power λ_i^{-4}.

Again, let k_1 be the momentum of the gluon that connect the two crossed vertices, and suppose k_1 is the larger loop momentum. It must then flow out from the short-distance vertex on the left, and may flow to the short-distance vertex on the right either along the double line at the top, or down to the P_3 line along the vertical gluon of the figure, and from there to the hard vertex on the right.

From our observations above, we need only do power counting for the remaining loop, k_2, to check for double poles. If the vertical gluon is virtual, the k_2 loop flows through the right-hand vertex and the vertical gluon line. Power counting for this loop depends on how the k_1 loop momentum flows. If k_1 flows along the top double line, we find $p_2 = 3$, while if k_1 flows down to P_3 along the virtual gluon, $p_2 = 2$. In both cases $p_2 < 4$, and the k_2 loop cannot produce an independent logarithmic divergence.

The power counting is a bit different if k_2 describes a gluon in the final state. Since k_2 is the softer gluon, k_1 cannot flow (backwards) through the k_2 gluon, but must flow only along the double line on top. The power counting for the softer line then again gives $p_2 = 2$.

Finally, if k_2 defines the harder of the two gluon momenta, we readily verify that the k_1 loop is infrared finite. In summary, diagram (IV) cannot produce a double pole in dimensional regularization.

In fact, diagram (IV) is the only diagram in Fig. 6 whose individual cuts lack a double pole. We now show, however, that for all of the remaining diagrams except for (I), the real parts of the residues of such double poles cancel in the sum over allowed cuts (final states) for each diagram. Imaginary double poles, of course, cancel when diagrams are combined with their conjugates. We will find a real double infrared pole from diagram (I).

Diagram (V): Let k_1 be the momentum of the gluon connecting the field-strength vertices, and k_2 the momentum of the gluon exchanged between the active pair and spectator P_3. From the power counting rules described above, it is clear that a double pole is produced by taking k_1 as the softer loop momentum. There are two final states to consider, one for which the gluon k_2 is virtual, and the other in which it is "real," that is, it appears in the final state.

Suppose that gluon k_2 is virtual. Taking the $\lambda_1 \to 0$ limit, the k_2 integral becomes the same NLO expression as in Eq. (12) above [for diagram (V) it is actually the complex conjugate]. As in that case, there are two contributions, associated with poles in the complex k_2^- plane at $k_2^2 = 0$ and $P\cdot k_2 = 0$. The former is purely real, the latter purely imaginary. When combined with the k_1 integral, they both produce $1/\varepsilon^2$ contributions in dimensional regularization. The imaginary pole, of course, cancels against the complex conjugate diagram. This leaves the real double pole, associated with an on-shell gluon k_2. This singularity cancels against the final state in which the gluon k_2 is real, point-by-point in the remaining momentum integrals [16].

Diagram (VI): In diagram (VI) double poles arise from a momentum configuration that is complementary to that of diagram (V). By analogy to the latter, we choose k_2 as the gluon attaching the active pair with P_3, and k_1 the remaining gluon, emitted from the field-strength vertex on the left of the diagram. The double pole then arises by taking k_2 as the softer loop momentum. At fixed values of k_1, however, the infrared poles arising from the k_2 integral cancel just as in the NLO case. Again, no double pole survives when diagram (VI) is added to its complex conjugate.

Diagram (III): In diagram (III), there are actually two relevant loop assignments for which the softer loop has logarithmic power counting. To describe them, we denote the momentum flowing out of the field-strength vertex on the left as k_1, and the momentum flowing into the field-strength vertex on the right as k_2. The momentum of the gluon attached to the P_3 (middle) line is then $k_2 - k_1$ (flowing up). The double logarithmic scalings are then $\lambda_1 \gg \lambda_2$ and $\lambda_1 \sim \lambda_2 \gg \lambda_2 - \lambda_1$. In the latter case, the larger momentum flows out of the active-pair eikonal and back, and in the former case, it flows down to the P_3 eikonal line. Both cases correspond to double logarithmic power counting, and in the calculation of Ref. [16], both regions contributed to a real single pole.

The calculation of (III) was described in great detail in Ref. [16], and the leading, double poles were found to follow the same pattern as for diagrams (V) and (VI) above. That is, real double poles cancel between final states in which the gluon that attaches to the P_3 line is either real or virtual, leaving purely imaginary double poles only. The loop integrations that led to this result are the same as in our case, except that the spectator was taken massless, $P_3^2 = 0$. Relaxing this condition, it is straightforward to verify that the calculations follow exactly the same pattern as in [16], and that diagram (III) does not contribute a double pole after a sum over final states. It is worth noting that most of the complications of [16] result from going to the level of the subleading, real single pole.

Diagram (II): For diagram (II), the pattern is the same as for (V) and (VI): the real double poles are associated with on-shell gluons, which cancel, leaving only an imaginary double pole proportional to the result found at NLO in Eq. (30). The pattern is again exactly as in the case of a massless eikonal spectator [16].

Diagram (I): We are left with diagram (I) as the only remaining potential source of a real double pole. Diagram (I) is associated with final states that include one, two, or no gluons. Exactly as in the massless case [16], the final states with one or two gluons cancel against the corresponding contributions from NLO virtual diagrams with one or two gluon lines on shell. (Notice that two-loop virtual corrections do not contribute in the octet-to-singlet transition amplitude, $\mathcal{M}_2$.) This real/virtual cancellation, however, leaves the absolute square of the imaginary single-pole term of Eq. (23), identified in Fig. 5. Again, this contribution is proportional to P_3^2, and was hence absent in the massless case studied in [16]. The complete infrared-sensitive result thus takes the form

$$\mathcal{M}_2 \sim \frac{\alpha_s^2}{\varepsilon^2} v^2 \frac{(1-\bar{\beta}_S^2)^3}{\bar{\beta}_S^4}, \tag{35}$$

which exhibits a strong dependence on relative velocity.

We should, of course, emphasize that we have not evaluated the single poles in these diagrams. For massless spectators, these poles can be factorized as in Ref. [16], but in this case we may safely assume that like the double poles they will depend on the kinematics of heavy particles in the final state. In any case, having found uncanceled double poles, we have already demonstrated the infrared sensitivity of color transfer, independent of the structure of the single poles. In the following section, we discuss possible physical implications of these uncanceled poles and the consequent infrared sensitivity to color transfer in associated production.

V. COLOR TRANSFER IN HEAVY QUARKONIUM PRODUCTION

We have shown that the imaginary $1/\varepsilon$ NLO corrections in Eqs. (23) and (30) result in real contributions to the octet-to-singlet transition amplitude, $\mathcal{M}_2$, at NNLO. As illustrated in Eq. (35) these corrections are conveniently expressed in terms of $\bar{\beta}_S$, Eq. (19), which measures the relative velocity of the spectator and the pair, as in Eq. (20). We are naturally led to suggest that these infrared-sensitive corrections tend to increase the cross section for bound states, since we have found a new source of pairs with singlet color at small $\bar{\beta}_S$. This does not yet give us an estimate for its effect on the production cross sections for quarkonia. To make such an estimate, we rely on an analogy to the physical picture at the basis of the color-octet mechanism as it appears in NRQCD.

A. Estimating color transfer

Consider first the standard color-octet mechanism. In this case, a (real) infrared pole is associated with the transition from a color-octet to a color-singlet pair at NLO through an electric dipole transition [1]. Each such transition is associated with a factor of the active-pair relative momentum, v in the amplitude, and v^2 in the cross section. We can summarize this perturbative result as [15,18]

$$d\sigma^{(\mathrm{PT})}_{\mathrm{octet}} \sim d\hat{\sigma}_{e^+e^-\to Q\bar{Q}[S_8]}(p_H) \frac{1}{\varepsilon} \frac{\alpha_s}{\pi} v^2, \tag{36}$$

with p_H the momentum of the heavy quarkonium, which is identified with the momentum of the active pair. In NRQCD, such infrared poles are matched with (equivalently, factorized into) color-octet matrix elements, $\langle \mathcal{L}_8^H \rangle$, for the final-state quarkonium, H. In this notation, $\mathcal{L}$ denotes the orbital angular momentum of the relevant operator. For J/ψ and similar quarkonia, $L = 0$ operators give the largest contributions, which requires at least two electric dipole transitions. This produces a greater suppression of v^4 in the cross section, and hence the corresponding matrix element, $\langle {}^3\mathcal{S}_8^H \rangle$. We thus make the replacement

$$d\hat{\sigma}_{e^+e^-\to Q\bar{Q}[S_8]}(p_H) \frac{1}{\varepsilon} \frac{\alpha_s}{\pi} v^2 \to d\hat{\sigma}_{e^+e^-\to Q\bar{Q}[S_8]}(p_H) \langle {}^3\mathcal{S}_8^H \rangle, \tag{37}$$

in which the infrared-sensitive correction at NLO is

matched to the nonperturbative S-wave matrix element, even though the latter has different scaling in v.

Now consider the NNLO color-transfer cross section in associated production, including the square of the full $\bar{\beta}$ dependence at lowest order in v, given in Eq. (20). Corresponding to Eq. (36), we have

$$d\sigma^{(\mathrm{PT})}_{\mathrm{transfer}} \sim d\hat{\sigma}_{e^+e^-\to Q\bar{Q}[S_8]+Q'(\beta_S)}(p_H)\,\frac{1}{\varepsilon^2}\,\alpha_s^2 v^2\,\frac{(1-\bar{\beta}_S^2)^3}{\bar{\beta}_S^4}. \tag{38}$$

The kinematic enhancement in this cross section associated with small $\bar{\beta}_S$ is very strong whenever $\bar{\beta} \le \sqrt{v}$, corresponding to low relative spectator-active velocities. The quadratic v dependence here is just the square of the linear v in Eq. (22), which is the same as that of an electric dipole transition. As for the color-octet mechanism, however, we anticipate that two transitions proportional to the dipole moment (and hence to v) will be necessary to produce a color-singlet, S-wave quarkonium. In the associated production cross sections at hand, the anticipated v^4 suppression that is normally absorbed into the matrix element is compensated, at least in part, by the explicit factor $1/\bar{\beta}_S^4$. In effect, for color transfer the expansion in v alone is replaced by an expansion in $v/\bar{\beta}$.

With our analogy in mind, it seems natural to replace the factor $\alpha_s^2 v^2/\varepsilon^2$ in (38) by the same octet matrix element as in (37). In making such a replacement, we are assuming that for color transfer it costs the same overall factor of v^4 as in the color-octet mechanism to produce an S-wave, color-singlet state for the active pair, and also that once the active pair is in a color-singlet state, it evolves independently of the spectator. We thus summarize our estimate of the full cross section for color transfer by

$$\begin{aligned} d\sigma^{\mathrm{tot}}_{e^+e^-\to H+X}(p_H) \sim{}& d\hat{\sigma}_{e^+e^-\to Q\bar{Q}[S_1]+Q'(\beta_S)}(p_H)\langle {}^3\mathcal{S}_1^H\rangle \\ &+ d\hat{\sigma}_{e^+e^-\to Q\bar{Q}[S_8]+Q'(\beta_S)}(p_H) \\ &\times \frac{\langle {}^3\mathcal{S}_8^H\rangle}{\bar{\beta}_S^4}(1-\bar{\beta}_S^2)^3. \end{aligned} \tag{39}$$

We emphasize that our arguments give this expression at best a heuristic justification, although we consider it a conservative estimate of the color-transfer contribution to associated production. We do not rule out the possibility that yet higher orders might lead to greater enhancement in $\bar{\beta}_S$, but we leave this to further investigation. Another approach to estimate color transfer in the velocity-ordered region is based on the observation that the active pair is not truly on shell, but should be treated according to pNRQCD methods [3,20]. The transverse momentum integrals that result in $1/\varepsilon$ poles in Eq. (12), for example, would then be replaced by logarithms of the bound-state relative velocity. In any case, to get a better idea of the role of color transfer, we should compare the sizes of the individual singlet and octet hard-scattering functions in Eq. (39), as they appear in the three-particle phase space of the heavy quarkonium and the associated pair. We turn now to this discussion.

B. Comparison of octet and singlet hard scattering

The color-transfer mechanism is most relevant to the kinematic region where the active heavy quark pair is in close vicinity with another heavy (anti)quark. As observed above, color transfer could significantly affect the rate of heavy quarkonium associated production, such as $e^+e^- \to J/\psi + c\bar{c} + X$, when the collision energy $\sqrt{s}$ is not too much higher than the mass threshold, $4m$, and the cross section is dominated by the region of phase space where one of the spectator heavy quarks is close to the active heavy quark pair. In addition, the mechanism should also have a strong effect on the size of the input distribution of heavy quark fragmentation functions, e.g., $D_{c\to J/\psi}(z, \mu_0, m)$, when the fragmentation scale μ_0 is close to $3m$. In either case, the radiation of light quanta will tend to decrease the effective s, and make it easier to produce spectators at low $\bar{\beta}$.

At collision energy $\sqrt{s} = 10.6$ GeV, as seen by the BELLE and *BABAR* collaborations, both heavy spectators in J/ψ associated production can be highly relativistic if the two pairs carry all the energy. We will find evidence in this subsection that even in this case the influence of the color-transfer mechanism on J/ψ production in association with $c\bar{c}$ could still be significant.

From Eq. (2), the lowest-order inclusive prompt production of a heavy quarkonium with an additional $Q\bar{Q}$ in NRQCD is given by

$$\begin{aligned} \sigma^{\mathrm{LO}}_{e^+e^-\to H+Q\bar{Q}}(s) = {}& \hat{\sigma}_{e^+e^-\to Q\bar{Q}[S_1]+Q'\bar{Q}'}(s)\langle {}^3\mathcal{S}_1^H\rangle \\ &+ \hat{\sigma}_{e^+e^-\to Q\bar{Q}[S_8]+Q'\bar{Q}'}(s)\langle {}^3\mathcal{S}_8^H\rangle. \end{aligned} \tag{40}$$

Although the direct octet contribution from ${}^3\mathcal{S}$ to the J/ψ production rate at $\sqrt{s} = 10.6$ GeV is only about 3% of the singlet contribution [21], the production rate, or coefficient function, for the active heavy quark pair is actually much higher for the octet mode than for the singlet, $\hat{\sigma}_{e^+e^-\to c\bar{c}[S_8]+c'\bar{c}'}(s) \gg \hat{\sigma}_{e^+e^-\to c\bar{c}[S_1]+c'\bar{c}'}(s)$. The octet mode is suppressed because the octet NRQCD matrix element $\langle {}^3\mathcal{S}_8^{J/\psi}\rangle$ is much smaller than the singlet matrix element $\langle {}^3\mathcal{S}_1^{J/\psi}\rangle$, by about 2 orders of magnitude [2]. In the estimate we have given above, Eq. (39), however, the contribution via the color-transfer mechanism could be very significant if the enhancement factor in $\bar{\beta}_S$ compensates for the suppression of the octet matrix element relative to the singlet.

The inclusive rate of charmonium production associated with an additional pair of heavy quarks in e^+e^- annihilation has been studied extensively in the NRQCD formalism at both LO [21,22] and NLO [14]. The LO analytic expression for the singlet production of various charmonium states in terms of the variable $z = 2E_{c\bar{c}}/\sqrt{s}$ is available [21,22], while numerical results for the inclusive rate are available for the NLO contribution [14]. To better understand the contributions to the inclusive rate of prompt J/ψ production from different parts of phase space, we express

the rate in terms of a phase space integration over the invariant masses of the active heavy quark pair and the heavy spectator (anti)quark:

$$s_3 \equiv (P + P_3)^2, \qquad s_4 \equiv (P + P_4)^2, \tag{41}$$

with $P^2 = (2m)^2$ and $P_3^2 = P_4^2 = m^2$. We denote the total squared collision energy by $s = (P + P_3 + P_4)^2$. The LO perturbative coefficient functions (or, at this order, the partonic cross sections to produce the state $Q\bar{Q}[S_n]$) in Eq. (40) are given by

$$\begin{aligned} d\hat{\sigma}_{e^+e^-\to Q\bar{Q}[S_n]+Q'\bar{Q}'}(s) &= \frac{1}{2s}\frac{1}{3}\frac{1}{c_n}\bar{\sum_\lambda}|\mathrm{Tr}[\mathcal{A}_{e^+e^-\to Q^i(P/2)\bar{Q}^j(P/2)+Q'\bar{Q}'}\mathcal{P}_{1\mu}]\epsilon_\lambda^\mu(P)\langle 3i\bar{3}j|n\rangle|^2 \frac{d^3P}{(2\pi)^3 2E_{Q\bar{Q}}}\frac{d^3P_3}{(2\pi)^3 2E_{Q'}} \\ &\quad \times \frac{d^3P_4}{(2\pi)^3 2E_{\bar{Q}'}}(2\pi)^4\delta^4(P_{e^+} + P_{e^-} - P - P_3 - P_4) \\ &= \sigma_0 e_c^2 \frac{\alpha_s(s)^2}{12s^2}\left(-g_{\mu\nu}W_{(n)}^{\mu\nu}(s, s_3, s_4, m)\right)\theta(\Phi(s, s_3, s_4, m))ds_3ds_4, \end{aligned} \tag{42}$$

where $n = 1$ or 8, $c_n = 2N_c$ or $N_c^2 - 1$, and $\langle 3i\bar{3}j|n\rangle = \delta_{ij}/\sqrt{N_c}$ or $\sqrt{2}(T^a)_{ji}$ for the singlet and octet contributions, respectively. The overall factor $1/3 = 1/(2J + 1)$ reflects $J = 1$, the spin of the active $Q\bar{Q}$ pair. In the trace, the projection operator for a spin-1 $Q\bar{Q}$ pair is $\mathcal{P}_1^\mu = (\gamma \cdot P/2 - m)\gamma^\mu(\gamma \cdot P/2 + m)/\sqrt{8m^3}$ [23]. In the second equation in Eq. (42), $\sigma_0 = 4\pi\alpha_{\mathrm{em}}^2/3s$, and $e_c = 2/3$ is the charm quark fractional charge. Finally, explicit forms for the hadronic tensor $W_{(n)}^{\mu\nu}$ with $n = 1, 8$ and the phase space constraint $\Phi(s, s_3, s_4, m)$ are given in the Appendix.

In Fig. 7, we show the integrand of the s_3s_4 integration for the production rate $\hat{\sigma}_{e^+e^-\to Q\bar{Q}(n)+Q'\bar{Q}'}(s)$ defined in Eq. (42) with an active heavy quark pair in a singlet (left panel) and octet (right panel) color state. To generate the figures in Fig. 7, we used $\sqrt{s} = 10.6$ GeV, $m = 1.5$ GeV. The units for the vertical axes are pb/GeV^3. After integrating over the phase space of s_3 and s_4, multiplying by the same singlet NRQCD matrix element for J/ψ production, $\langle {}^3S_1\rangle = \langle \mathcal{O}_1^{\mathrm{J}/\psi}({}^3_1)\rangle = 1.16$ GeV^3, and using the same value of α_s used in Ref. [21], we obtain the same 148 fb cross section from the direct singlet contribution. We also find that the direct octet contribution is about 3% of the singlet contribution. Since the octet NRQCD matrix element to J/ψ, $\langle {}^3S_8\rangle = \langle \mathcal{O}_8^{\mathrm{J}/\psi}({}^3_1)\rangle = 1.06 \times 10^{-2}$ GeV^3, is about 100 times smaller than the corresponding singlet matrix element, it is clear that before multiplying by the NRQCD matrix elements, as shown in Fig. 7, the production rate for a color-octet active heavy quark pair is larger than the rate of producing a singlet pair everywhere in the phase space including the region where the invariant mass s_3 or s_4 is small. The octet production rate is much higher than the singlet rate when both s_3 and s_4 are large because the active quark and the antiquark of the singlet contribution at this order cannot come from a pair of heavy quarks that originate from either the same virtual photon or gluon. With an additional enhancement factor from the color-transfer mechanism, the octet contribution will also peak in the region where the invariant, s_3 or s_4, is small. At the same time, the enhancement in the color-octet coefficient functions away from these regions seems to imply that the cross section for color transfer will decay less rapidly than might be expected on the basis of the explicit factors of $\bar{\beta}_S$ alone in Eq. (39).

VI. HIGH-ENERGY BEHAVIOR AND FRAGMENTATION

Equation (39) estimates the effect of color transfer on the production cross section as an energy-independent factor times a perturbative cross section. In this section, we show why this is a natural assumption, even though the

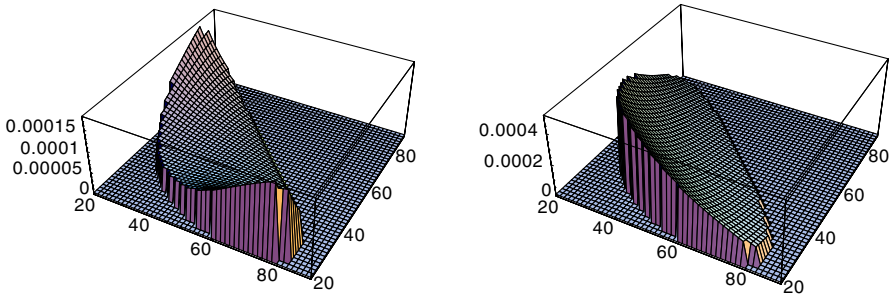

FIG. 7 (color online). The integrand, in pb/GeV^3, of the s_3s_4 integration for the production rate of an active heavy quark pair, defined in Eq. (42), with the pair in a color-singlet (left panel) or a color-octet (right panel) state.

color-transfer process acts in a restricted region of phase space, specified by Eq. (21). It is necessary to check that color transfer survives in the high-energy limit, and that it can play a role in the fragmentation of heavy flavor at high transverse momentum.

A. Color transfer in fragmentation

Figure 8 shows a typical fragmentation process for associated production at lowest order, in cut diagram notation. To be definite, we discuss fragmentation in leptonic annihilation, as in Fig. 1. The underlying factorization that justifies fragmentation analysis extends as well to hadronic scattering, as shown in Ref. [17].

The shaded circles in Fig. 8 represent, as above, short-distance functions, now with all propagators off shell by Q^2, where Q is the center-of-mass energy. We assume all $P_i^2 = m^2$, taking both heavy-flavor masses equal. All propagators enclosed within the dashed lines are then off shell by at least $4m^2$, and remain short-distance contributions from the point of view of NRQCD, as in Fig. 2.

From our previous considerations, we know that the color-transfer process arises from truly infrared gluons, and will thus not affect the propagators of lines that are off shell by the scales m or Q. Rather, the infrared enhancement will be associated with factors that depend sensitively on the relative velocities of the external lines. We will now show that color transfer is leading power in Q, although it will not appear in logarithmic enhancements associated with large relative velocities between P_3 and P_1 or P_2.

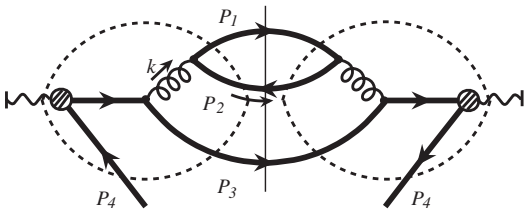

FIG. 8. Representative fragmentation contribution to associated production, discussed in the text. The dashed lines represent contributions that would be included in the short-distance function at low energies, as in Fig. 2.

Let us denote by $d\tau_n(Q^\mu)$ differential n-particle phase space at total four-momentum Q^μ. The inclusive associated-pair production cross section at total momentum $Q^\mu \equiv (Q, \vec{0})$ can then be represented as

$$\int d\tau_4(Q^\mu)\frac{d\sigma(\{P_i\})}{d\tau_4} = \frac{1}{2Q^2}\int \frac{d^3\vec{P}_4}{2(2\pi)^3\sqrt{\vec{P}_4^2+m^2}} d\tau_3(Q^\mu - P_4^\mu)|M_4(Q, P_1 \ldots P_3)|^2$$
$$= \frac{1}{8(2\pi)^3 Q^3}\int d\Omega_4 \int ds_{123}\sqrt{\left(\frac{Q^2+m^2-s_{123}}{2Q}\right)^2 - m^2}\int d\tau_3(Q^\mu - P_4^\mu)|M_4(Q, P_1 \ldots P_3)|^2. \quad (43)$$

Here and below, we introduce the notation $s_{ij\ldots} \equiv (P_i + P_j + \ldots)^2$, while M_n is the amplitude for the production of n heavy particles. A sum over final-state spins is assumed. The vector P_4 is on shell, with the direction of its spatial momentum specified by the angular integral, $\int d\Omega_4$.

At high energy and fixed invariant mass $\sqrt{s_{123}}$ of the three-particle (1,2,3) system, the amplitude factorizes into a hard function for single-pair production multiplied by an integral that describes the fragmentation of a parent (anti)quark into a(n) (anti)quark plus a pair, as in Fig. 8. In the high-energy limit for fixed s_{123}, the corresponding squared amplitude integrated over three-particle phase space then factorizes into the squared amplitude for two-particle production, times logarithmic integrals characteristic of fragmentation. Suppressing dependence on the relative angles of the $\vec{P}_i$, $i = 1, 2, 3$, the remaining integrals in three-particle phase space appear in the factorized expression as

$$\int d\tau_3(Q^\mu - P_4^\mu)|M_4(Q, P_1 \ldots P_3)|^2$$
$$\sim |M_2(P_4, \overline{Q - P_4})|^2 \int d\tau_3(Q^\mu - P_4^\mu)\frac{1}{s_{123}s_{12}}$$
$$\sim M_2(P_4, \overline{Q - P_4})|^2 \frac{1}{s_{123}^2}\int_{4m^2} ds_{23}\frac{ds_{12}}{s_{12}}$$
$$\times \theta(s_{123} - s_{12} - s_{23} - 3m^2), \quad (44)$$

where $\overline{Q - P_4}$ denotes an on-shell four-vector recoiling against P_4. The kinematic dependence on the right-hand side of the first relation of (44) comes from the denominators of the squared propagators shown in Fig. 8, which give $1/s_{12}^2 s_{123}^2$, multiplied by momentum factors from the spinor algebra, which give an additional factor in the numerator of $s_{12}s_{123}$. A remaining, overall factor of $\gamma \cdot (Q - P_4)$ has been absorbed into the squared two-particle matrix element $|M_2|^2$ in the expression. In these terms, three-particle phase space reduces to an infrared finite, but logarithmic, integral over the squared invariant mass of the (1,2) pair, times a free integral over the squared invariant mass of the (2,3) pair. The theta function restriction on s_{12} and s_{23} reflects an identity for three-particle phase space: $s_{123} = s_{12} + s_{23} + s_{13} + 3m^2$.

At lowest order (Fig. 8, for example), the s_{12} integral in Eq. (44) behaves as $s_{123}\ln(s_{123}/4m^2)$. This leads, in turn, to an additional logarithmic integral over s_{123} in Eq. (43). These are standard logarithmic enhancements associated with the evolution of a fragmentation function. If we demand, however, that one of the two pairs of Fig. 8 form a heavy quarkonium, we will restrict either s_{23}, for the lowest-order color-singlet contribution, or s_{12}, for the lowest-order color octet, to remain close to $4m^2$. The available phase space for the formation of the heavy quarkonium is set by the requirement that the active pair

should have relative momentum of the order mv. This limitation on phase space is taken into account in NRQCD matrix elements, which always include a scaling of order v^3. In lowest-order singlet production, this limitation would be placed on s_{23}, which eliminates both of the logarithmic enhancements identified above. For the lowest-order octet mechanism, the restriction can be placed on s_{12}, and we may still generate a single logarithm from the integral over s_{123}.

We can now consider infrared-sensitive NNLO color-transfer corrections to Fig. 8. In this case, we generate additional dependence on the relative velocities of the heavy particles, and hence on the invariants s_{23} and s_{12}. As we have seen, this dependence arises from the square of the NLO correction given in Eq. (23), and it decreases rapidly with increasing relative velocities between the active pair and the spectator. Thus, such a correction suppresses the cross section when s_{123} grows to a multiple of $9m^2$.

To be specific, recalling the definition of the variable $\bar{\beta}_S$ in Eqs. (10) and (19), and neglecting v compared to $\bar{\beta}_S$, we find an additional s_{123} dependence in the integrand of Eq. (44),

$$\frac{(1-\bar{\beta}_S^2)^3}{\bar{\beta}_S^4}\int ds_{23}\frac{ds_{12}}{s_{12}}\theta(s_{123}-s_{12}-s_{23}-3m^2) = \left[\frac{64m^6}{(s_{123}-9m^2)(s_{123}-5m^2)(s_{123}-m^2)}\right]^2 \times \int ds_{23}\frac{ds_{12}}{s_{12}}\theta(s_{123}-s_{12}-s_{23}-3m^2), \quad (45)$$

where the lower limit of the s_{123} integral will be set by $\bar{\beta}_S > v$, and where there is a rapid decrease for $s_{123} \gg m^2$. As with the color-octet mechanism for this lowest-order process, the (1,2) pair forms the bound state, and we anticipate an overall suppression in the s_{12} integral of v^3 on dimensional grounds. Although nonlogarithmic, the s_{123} integral remains leading power in Q, with no further suppression by powers of v.

B. Light quarks and polarization

By referring to Fig. 8, we can make a very simple observation relevant to the comparison of the associated production cross section for heavy quarkonia with heavy flavors compared to light flavors only. The leading power behavior for the production of single heavy quark pairs in close proximity in phase space is due entirely to fragmentation. The color-transfer contribution for fragmentation diagrams as shown in the figure is present only for associated production, since light quarks will unavoidably have much larger relative velocities, $\bar{\beta}_S$. At lowest order, then, we would expect the fragmentation of a light quark to a heavy quarkonium to proceed only through the color-octet matrix element. For leptonic annihilation, in particular, where gluon fragmentation is yet higher order in α_s, the color-transfer process affects heavy-flavor associated production only.

Related considerations apply to the prediction of transverse polarizations for heavy quarkonia produced from gluon fragmentation [10,11,24]. It is easy to check that the color-transfer process does not give such a prediction. The color transfer itself respects the spin of the pair, which reflects the polarization of a collinear gluon in the fragmentation process (the gluon of invariant mass s_{12} in Fig. 8). Indeed, at high energies, the polarization of this gluon naturally includes large longitudinal components. A further study of this issue is clearly in order.

VII. SUMMARY AND CONCLUSION

The color-transfer process that we have described above provides a new viewpoint on the hadronization of heavy quarks in associated production. In color transfer, the pair produced from a single gluon can be transformed from octet-to-singlet representation by the field of an open (anti)quark that is at sufficiently low relative velocity. We can picture it as a process that catalyzes quarkonium production when another heavy quark is nearby in phase space. Experimental confirmation of such a process could provide a significant tool to study dynamical processes in quantum chromodynamics. Color transfer complements the standard picture of hadronization through string breaking, in which color neutral pairs are formed from quarks and antiquarks that originate from separate virtual gluons [25]. The latter is leading power in the number of colors, and color transfer is hence nonleading in this expansion.

We have shown that, in perturbation theory, color transfer appears first at NNLO. At this level, it is positive, but not infrared safe. Although nonperturbative it cannot be described in terms of the matrix elements of NRQCD in general. Without experimental input, we are not yet in the position to give a realistic estimate of its importance.

Color transfer could be part of the explanation of well-known anomalies in comparisons of data to NRQCD predictions [10,13], and it may be possible to confirm its role through a number of qualitative predictions that flow naturally from the perturbative reasoning above.

First, we would expect color transfer to produce phase space distributions that are peaked at small relative invariant mass between the heavy quarkonium and closest open heavy flavor in associated production. For example, an experimental signal of this effect would be an enhancement of J/ψ production relative to NRQCD estimates at low values of the invariant masses of $J/\psi - D$ and $J/\psi - \bar{D}$ pairs. At high energies, a similar effect should be found both in $\Upsilon - D$ and $\Upsilon - B$ systems. Second, if color transfer enhances associated production at large transverse momenta, it could also help explain the observed polarizations of heavy quarkonia.

A Dalitz plot analysis of quarkonium/open flavor final states at B factory energies could show enhancements on

the low pair mass corners. At the same time, our analysis suggests that, in the interior of such a Dalitz plot, an NRQCD analysis based on the color-singlet mechanism should succeed. In general, semi-inclusive measurements of the distribution of heavy flavor in final states could even enable us to probe the time evolution of flavor, momentum, and spin in the formation of the final state. This would complement the inclusive viewpoint which is built into the important NRQCD calculations of Refs. [12,14].

Color transfer is distinct from, yet in some ways analogous to, the usual NRQCD color-octet mechanism, which relies on soft gluon radiation. It is kinematically dependent on soft gluon exchange with other particles in the final state, and hence is not "universal" in the sense of NRQCD. On the other hand, the effect decreases with relative transverse momentum, and hence does not spoil high-p_T factorization, as described, for example, in [16]. Similarly, it does not occur at all through exchanges with massless particles, and hence is specific to associated production with heavy flavor.

In conclusion, although many issues remain to be studied, the color-transfer mechanism suggests a number of phenomenological signals, which should make it possible to test its relevance to associated production. If it does pass these experimental tests, it may offer insight into the dynamics of color in hadronization.

ACKNOWLEDGMENTS

We thank Geoff Bodwin for many useful discussions on factorization. This work was supported in part by the National Science Foundation, Grant No. PHY-0354776, No. PHY-0354822 and No. PHY-0653342, by the U.S. Department of Energy under Grant No. DE-FG02-87ER40371 and No. DE-FG02-01ER41195 and Contract No. DE-AC02-06CH11357, and in part by the Argonne University of Chicago Joint Theory Institute (JTI) Grant No. 03921-07-137.

APPENDIX: LOWEST-ORDER MATRIX ELEMENTS FOR HEAVY QUARKONIUM ASSOCIATED PRODUCTION

In this appendix, we provide the leading-order squared matrix elements, $-g_{\mu\nu}W^{\mu\nu}_{(n)}$, that appear in Eq. (42), for producing an active pair of heavy quark and antiquark of mass m, in association with another heavy quark pair of the same mass. For the active pair in a singlet color state, $n = 1$, we have

$$
\begin{aligned}
-g_{\mu\nu}W^{\mu\nu}_{(1)} = \frac{64}{27m}\Bigg\{ & \frac{2}{(m^2-s_3)^2(m^2-s_4)^2(-2m^2+s_3+s_4-2s)^2}[132m^{10}+2(136s-101(s_3+s_4))m^8 \\
& +4(7s_3^2+108s_4s_3+7s_4^2+240s^2-58(s_3+s_4)s)m^6-(31s_3^3+149s_4s_3^2+149s_4^2s_3+31s_4^3-380s^3 \\
& +316(s_3+s_4)s^2-9(9s_3^2-2s_4s_3+9s_4^2)s)m^4+(s_3^4+56s_4s_3^3+98s_4^2s_3^2+56s_4^3s_3+s_4^4+32s^4 \\
& -60(s_3+s_4)s^3+12(3s_3^2-2s_4s_3+3s_4^2)s^2-(s_3+s_4)(s_3^2-10s_4s_3+s_4^2)s)m^2+s_3s_4(-9s_3^3-25s_4s_3^2 \\
& -25s_4^2s_3-9s_4^3-4s^3+4(s_3+s_4)s^2+(9s_3^2+14s_4s_3+9s_4^2)s)] \\
& -\frac{1}{(m^2-s_3)^4}[64m^6+(41s_3+9s_4+47s)m^4 \\
& +2s_3(s-5(s_3+s_4))m^2+s_3^2(s_3+s_4-s)+\frac{2(m^2-s_3)}{-2m^2+s_3+s_4-2s}[257m^6+3(2s_3-7s_4+54s)m^4 \\
& -(7s_3^2+36s_4s_3+10s_4^2-16s^2+2(s_3+7s_4)s)m^2+s_3s_4(s_3+2s_4-2s)] \\
& +\frac{4(m^2-s_3)^2}{(-2m^2+s_3+s_4-2s)^2}[160m^6+3(5s_3-15s_4+37s)m^4-2(5s_3^2+14s_4s_3-2ss_3+7s_4^2-4s^2+5s_4s)m^2 \\
& +(2s_3^2+4s_4s_3+3s_4^2)(s_3+s_4-s)]] \\
& -\frac{1}{(m^2-s_4)^4}[64m^6+(9s_3+41s_4+47s)m^4+2s_4(s-5(s_3+s_4))m^2 \\
& +s_4^2(s_3+s_4-s)+\frac{2(m^2-s_4)}{-2m^2+s_3+s_4-2s}[257m^6+(6(s_4+27s)-21s_3)m^4-(10s_3^2+36s_4s_3+7s_4^2-16s^2 \\
& +2(7s_3+s_4)s)m^2+s_3s_4(2s_3+s_4-2s)]+\frac{4(m^2-s_4)^2}{(-2m^2+s_3+s_4-2s)^2}[160m^6+(-45s_3+15s_4+111s)m^4 \\
& -2(7s_3^2+14s_4s_3+5ss_3+5s_4^2-4s^2-2s_4s)m^2+(3s_3^2+4s_4s_3+2s_4^2)(s_3+s_4-s)]]\Bigg\}. \qquad \text{(A1)}
\end{aligned}
$$

For the pair in an octet color state, $n = 8$, we have

$$
\begin{aligned}
-g_{\mu\nu}W^{\mu\nu}_{(8)} = \frac{1}{9m(m^2-s_3)^4(m^2-s_4)^4}\Big\{ & 1594m^{14} - 4588s_3m^{12} - 4588s_4m^{12} + 4285s_3^2m^{10} + 4285s_4^2m^{10} + 13670s_3s_4m^{10} \\
& - 1961s_3^3m^8 - 1961s_4^3m^8 - 12723s_3s_4^2m^8 - 12723s_3^2s_4m^8 + 553s_3^4m^6 + 553s_4^4m^6 + 5699s_3s_4^3m^6 \\
& + 10316s_3^2s_4^2m^6 + 5699s_3^3s_4m^6 - 75s_3^5m^4 - 75s_4^5m^4 - 1417s_3s_4^4m^4 - 3760s_3^2s_4^3m^4 - 3760s_3^3s_4^2m^4 \\
& - 1417s_3^4s_4m^4 + 127s_3s_4^5m^2 + 791s_3^2s_4^4m^2 + 846s_3^3s_4^3m^2 + 791s_3^4s_4^2m^2 + 127s_3^5s_4m^2 - 61s_3^2s_4^5 - 137s_3^3s_4^4 \\
& - 137s_3^4s_4^3 - 61s_3^5s_4^2 + \frac{4(m^2-s_3)(m^2-s_4)}{-2m^2+s_3+s_4-2s}[478m^{12} - 1130(s_3+s_4)m^{10} + (619s_3^2 + 3084s_4s_3 + 619s_4^2)m^8 \\
& - 4(s_3+s_4)(74s_3^2 + 383s_4s_3 + 74s_4^2)m^6 + 2(84s_3^4 + 256s_4s_3^3 + 441s_4^2s_3^2 + 256s_4^3s_3 + 84s_4^4)m^4 \\
& - (s_3+s_4)(19s_3^4 + 110s_4s_3^3 + 40s_4^2s_3^2 + 110s_4^3s_3 + 19s_4^4)m^2 + s_3s_4(7s_3^4 + 21s_4s_3^3 + 6s_4^2s_3^2 + 21s_4^3s_3 + 7s_4^4)] \\
& + \frac{4(m^2-s_3)^2(m^2-s_4)^2}{(-2m^2+s_3+s_4-2s)^2}[244m^{10} - 458(s_3+s_4)m^8 + 4(17s_3^2 + 304s_4s_3 + 17s_4^2)m^6 \\
& - 2(s_3+s_4)(57s_3^2 + 136s_4s_3 + 57s_4^2)m^4 + 2(19s_3^4 + 52s_4s_3^3 + 52s_4^2s_3^2 + 52s_4^3s_3 + 19s_4^4)m^2 \\
& - (s_3+s_4)(3s_3^4 + 8s_4s_3^3 + 12s_4^2s_3^2 + 8s_4^3s_3 + 3s_4^4)] + \frac{2(7m^2-3s_3)(m^2-s_3)^2(7m^2-3s_4)(m^2-s_4)^2s^2}{m^2} \\
& + \frac{9s_3^3s_4^3(6m^4 + 2(s_3+s_4)m^2 + s_3^2 + s_4^2)}{m^2} + \frac{2s}{m^2}[252m^{14} - 677(s_3+s_4)m^{12} + (301s_3^2 + 2438s_4s_3 + 301s_4^2)m^{10} \\
& + (s_3+s_4)(173s_3^2 - 2185s_4s_3 + 173s_4^2)m^8 + (-97s_3^4 + 410s_4s_3^3 + 1946s_4^2s_3^2 + 410s_4^3s_3 - 97s_4^4)m^6 \\
& + s_3s_4(s_3+s_4)(33s_3^2 - 581s_4s_3 + 33s_4^2)m^4 + s_3^2s_4^2(25s_3^2 + 166s_4s_3 + 25s_4^2)m^2 - 9s_3^3s_4^3(s_3+s_4)]\Big\}. \qquad \text{(A2)}
\end{aligned}
$$

The invariants in these expressions are defined as $s = (P + P_3 + P_4)^2$, $s_3 = (P + P_3)^2$, and $s_4 = (P + P_4)^2$, respectively.

The phase space integration of ds_3ds_4 in Eq. (42) is given by the condition $\Phi(s, s_3, s_4, m) \geq 0$, with the function [26]

$$
\begin{aligned}
\Phi(s, s_3, s_4, m) = {} & s_3s_4(6m^2 - s_3 - s_4 + s) \\
& + 3(s - m^2)(s_3 + s_4)m^2 \\
& - (s + 6m^2)(4s + m^2)m^2 \\
& + 2(9s + 4m^2)m^4. \qquad \text{(A3)}
\end{aligned}
$$

[1] G. T. Bodwin, E. Braaten, and G. P. Lepage, Phys. Rev. D **51**, 1125 (1995); **55**, 5853(E) (1997).

[2] N. Brambilla *et al.* (Quarkonium Working Group), arXiv:hep-ph/0412158.

[3] N. Brambilla, A. Pineda, J. Soto, and A. Vairo, Rev. Mod. Phys. **77**, 1423 (2005).

[4] J. P. Lansberg, Int. J. Mod. Phys. A **21**, 3857 (2006).

[5] N. Brambilla, A. Pineda, J. Soto, and A. Vairo, Nucl. Phys. **B566**, 275 (2000).

[6] M. E. Luke, A. V. Manohar, and I. Z. Rothstein, Phys. Rev. D **61**, 074025 (2000).

[7] A. H. Hoang, in *At the Frontier of Particle Physics/ Handbook of QCD*, edited by M. Shifman (World Scientific, Singapore, 2002), Vol. 4, p. 2215.

[8] G. C. Nayak, J. W. Qiu, and G. Sterman, Phys. Rev. Lett. **99**, 212001 (2007).

[9] F. Abe *et al.* (CDF Collaboration), Phys. Rev. Lett. **79**, 572 (1997); D. Acosta *et al.* (CDF Collaboration), Phys. Rev. D **71**, 032001 (2005); V. M. Abazov *et al.* (D0 Collaboration), Phys. Rev. Lett. **94**, 232001 (2005).

[10] A. A. Affolder *et al.* (CDF Collaboration), Phys. Rev. Lett. **85**, 2886 (2000); A. Abulencia *et al.* (CDF Collaboration), Phys. Rev. Lett. **99**, 132001 (2007).

[11] P. L. Cho and M. B. Wise, Phys. Lett. B **346**, 129 (1995); M. Beneke and I. Z. Rothstein, Phys. Lett. B **372**, 157 (1996); **389**, 769 (1996); M. Beneke and M. Kramer, Phys. Rev. D **55**, R5269 (1997); E. Braaten, B. A. Kniehl, and J. Lee, Phys. Rev. D **62**, 094005 (2000).

[12] P. Artoisenet, J. P. Lansberg, and F. Maltoni, Phys. Lett. B **653**, 60 (2007).

[13] K. Abe *et al.* (Belle Collaboration), Phys. Rev. Lett. **89**, 142001 (2002); B. Aubert *et al.* (*BABAR* Collaboration), Phys. Rev. D **72**, 031101 (2005).

[14] Y. J. Zhang and K. T. Chao, Phys. Rev. Lett. **98**, 092003 (2007).

[15] M. Kramer, Prog. Part. Nucl. Phys. **47**, 141 (2001); G. T. Bodwin, J. Korean Phys. Soc. **45**, S306 (2004).

[16] G. C. Nayak, J.-W. Qiu, and G. Sterman, Phys. Lett. B **613**, 45 (2005); Phys. Rev. D **72**, 114012 (2005).

[17] G. C. Nayak, J. W. Qiu, and G. Sterman, Phys. Rev. D **74**,

074007 (2006).

[18] E. Braaten, S. Fleming, and T. C. Yuan, Annu. Rev. Nucl. Part. Sci. **46**, 197 (1996); A. Petrelli, M. Cacciari, M. Greco, F. Maltoni, and M. L. Mangano, Nucl. Phys. **B514**, 245 (1998).

[19] G. Sterman, in *QCD and Beyond, Proceedings of 1995 Theoretical Advanced Study Institute (TASI95) Boulder, CO, 1995*, edited by D. E. Soper (World Scientific, Singapore, 1996).

[20] B. A. Kniehl, A. A. Penin, V. A. Smirnov, and M. Steinhauser, Nucl. Phys. **B635**, 357 (2002); M. Beneke, Y. Kiyo, and A. A. Penin, Phys. Lett. B **653**, 53 (2007).

[21] K. Y. Liu, Z. G. He, and K. T. Chao, Phys. Rev. D **69**, 094027 (2004); and references therein.

[22] V. V. Kiselev, A. K. Likhoded, and M. V. Shevlyagin, Phys. Lett. B **332**, 411 (1994); P. L. Cho and A. K. Leibovich, Phys. Rev. D **54**, 6690 (1996); F. Yuan, C. F. Qiao, and K. T. Chao, Phys. Rev. D **56**, 321 (1997).

[23] E. L. Berger and D. L. Jones, Phys. Rev. D **23**, 1521 (1981).

[24] S. Baek, P. Ko, J. Lee, and H. S. Song, Phys. Rev. D **55**, 6839 (1997).

[25] D. Amati and G. Veneziano, Phys. Lett. **83B**, 87 (1979); R. K. Ellis, W. J. Stirling, and B. R. Webber, *QCD and Collider Physics*, Camb. Monogr. Part. Phys. Nucl. Phys. Cosmol., Vol. 8 (Cambridge University Press, Cambridge, England, 1996).

[26] A. I. Davydychev and R. Delbourgo, J. Phys. A **37**, 4871 (2004).